MME 4499 – Mechanical Engineering Design Project

Torsional Stiffness Improvements on 4x Rowing Hulls

by

Fiona Mackenzie, Glen Norman, Katherine MacIsaac, Robyn Sugimoto

Report 4

Faculty Advisor: John Makaran

Date Submitted: April 4th, 2025

Executive Summary

Fluidesign manufactures high-end racing boats and is seeking to redesign the hull of their quad boat to meet competitive standards and improve performance for high-level racing. The current design has limitations in torsional and lateral stiffness. The redesign aims to narrow the gunnel dimensions to accommodate smaller double riggers, as well as to change the materials and layup to increase overall stiffness by 20%. Despite the narrower dimensions for the smaller riggers, the overall weight will be maintained, with a focus on enhancing both lateral and torsional stiffness.

The quad redesigning process has been divided into three different sections for testing. First, physical vibration tests were performed, involving impacting the current quad boat with a rubber mallet and using an accelerometer to measure the acceleration at different locations along the hull of the boat. With the collected data from this test, the highest deflections and harmonic frequencies were found and used to determine the locations of the weakest points along the hull, and where the boat requires changes to be made for stiffness improvements. These weak areas were found to be in the middle of the boat below the gunnels. Once the weak points were identified, a SolidWorks model replicating the hull was built, and SolidWorks simulations were performed, applying forces along the boat to replicate the forces applied in a row stroke.

The second section of testing was performed using SolidWorks, but first the hull had to be constructed with new dimensions. The first dimensional changes were made by adjusting the distance between the rigger rails from 572 to 457 mm, with a continuous smooth transition from the bottom of the hull to the gunnel. However, after multiple tests were run, it was discovered that the lateral stiffness was decreasing with these new dimensions, and therefore another dimensional change had to be made. The next iteration of dimensions still had the adjusted distance between the rigger rails from 572 to 457, but a slight bend was created in the transition between the bottom of the hull, and the gunnel was shortened to minimize the lateral deflection. The simulations were then run, and the displacement, as well as the z-axis rotation of the different hulls were measured, concluding that the final iteration was successful, and the lateral and torsional stiffness were increased, concluding that the simulations could then be performed on the hull to determine the materials that should be used.

For the third section of testing, the materials and material layup were determined. The material testing and selection process consisted of SolidWorks simulations and physical three-point bend tests. For the SolidWorks simulations, various carbon fiber layups were tested, where different weaves of carbon fiber were layered and aligned in various directions, comparing the new material layups to the original, with row stroke simulations. The main change that was made to the layup was the addition of reinforcement in an ‘X’ formation along the hull of the boat with a unidirectional weave, which added a significant amount of stiffness to the hull. The different carbon fiber weaves were selected from research, but they need to be confirmed with physical testing.

The second half of the third section material testing was physical three-point bend tests, this test was performed using different weaves and types of carbon fiber. The carbon fiber samples were infused with the epoxy resin from Fluidesign and three-point bend tests were performed on all of the samples. The

results from the three-point bend test helped to determine how the materials behave with the epoxy resin in the carbon fiber, assisting in the confirmation that the materials selected for the new layup are the best for increasing the torsional and lateral stiffness.

The overall cost of testing materials was $144.41, and with the budget of $800, there were no issues. The testing equipment purchased included a piezoelectric accelerometer, an Arduino kit with a 22-gauge shielded wire, beeswax, a Bluetooth accelerometer and a carbon fiber sample pack. All purchases made helped in the testing process and were necessary to be purchased. The cost of the new design increases with material costs from the original $1,192 to the new materials being $1,847. However, the new molds will have a significant change in the cost, with an estimated final cost of the entire new boat being about $21,847.

Overall, Fluidesign's quad boat hull redesign process has been a comprehensive and iterative experience, aimed at improving the boat's performance by enhancing both lateral and torsional stiffness. This project has been successful, increasing the lateral stiffness by approximately 50% and the torsional stiffness by over 300%. Through a combination of physical vibration tests, SolidWorks simulations, and material testing, the weakest points were determined in the original hull design and the new design was finalized. By adjusting dimensions, the final design successfully increased stiffness while maintaining the desired weight of 50 kg. Material testing further confirmed the effectiveness of the new carbon fiber layup, with a reinforced unidirectional weave providing significant improvements in both torsional and lateral stiffness. This three-section approach, incorporating both simulation and physical testing, ensures that the final hull design meets the competitive standards required for high-level racing while delivering enhanced performance on the water.

Table of Contents

List of Figures

List of Tables

Acknowledgements

We would like to thank Sam and Connor from Fluidesign for supporting us with our project.

We would also like to thank professors Dr. John Makaran, Dr. Harvey Shi, and Dr. Ben Hamilton for the guidance they provided through this project.

Nomenclature

FEA: Finite Element Analysis

Scull: Rowing race style where each rower has two oars.

Sweep: Rowing race style where each rower has one oar.

---

1. General Information

1.1 Problem Definition

Fluidesign is looking to improve their quad boat hull, aiming to get this product into a new market of competitive racing. Currently, their single and double boats have been optimized and are competing at international and Olympic levels. The current design of the quad boat's gunnels and carbon layup lacks torsional and lateral stiffness (see Figure 1**Error! Reference source not found.** for rowboat terminology). As a result of this, deflection is causing power from the rower to be lost, preventing the boat from reaching higher speeds. Through physical testing and FEA, improvements are to be made to these factors with a new model that optimizes stiffness while minimizing weight.

This project has been divided into 3 major objectives. The first step is a redesign of the quad hull. This section requires modification of the gunnel and flange area of the boat to minimize lateral deflection. Another goal of this section is to fit Fluidesign's double riggers to fit on the quad boats, allowing them to reduce their manufacturing requirements. To meet this requirement, the distance between the riggers and the sweep rails of the boat will need to be shorter to match the target dimensions (see **Error! Reference source not found.** and **Error! Reference source not found.**). This is accomplished using CAD and FEA analysis to determine feasibility.

The next step in remodeling uses FEA to model the carbon layup of the quad boat to increase stiffness. Given the current material data sheets, a custom layup can be created that will fit the required properties. Using the given CAD models and the new custom materials, the new layup will be modeled and used to test relevant loading cases for FEA. Using the layup as a baseline, the model can be adjusted to optimize stiffness and minimize weight. These versions will then be tested in FEA and compared with other layups. Finally, physical testing will be performed to determine the stiffness of different materials.

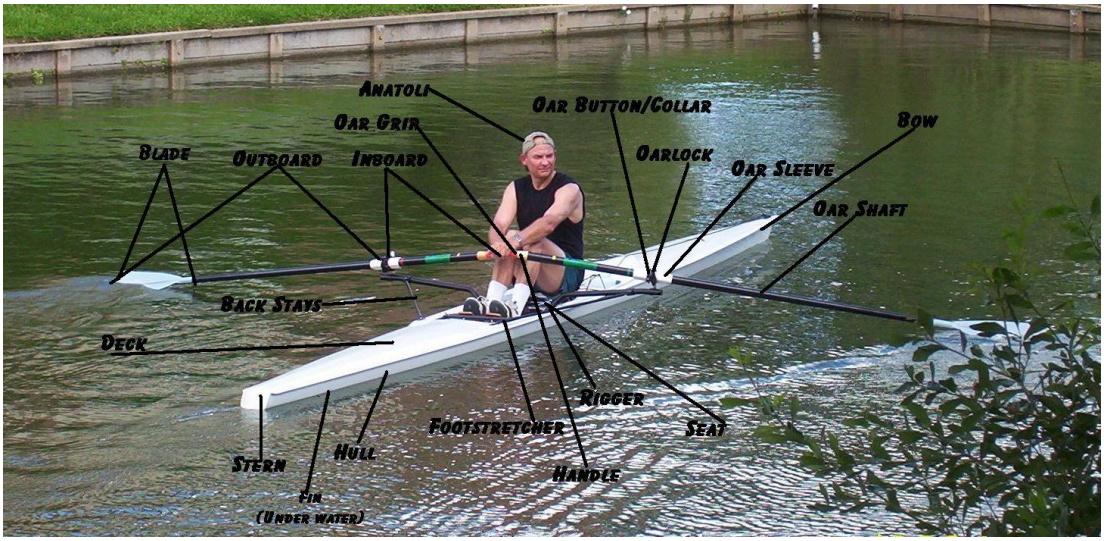

Figure 1. Rowboat terminology *Source:* *https://www.google.ca/url?sa=i&url=https%3A%2F%2Fwww.adirondackrowing.com%2Fshell-*

lingo%2F&psig=AOvVaw1uGQGKHJQg2KfSas4wv6V7&ust=1727457181721000&source=images&cd=vfe&opi=89978449&ved=0CBQQjRxqFwoTCMCfytCN4YgDFQAAAAAdAAAAA

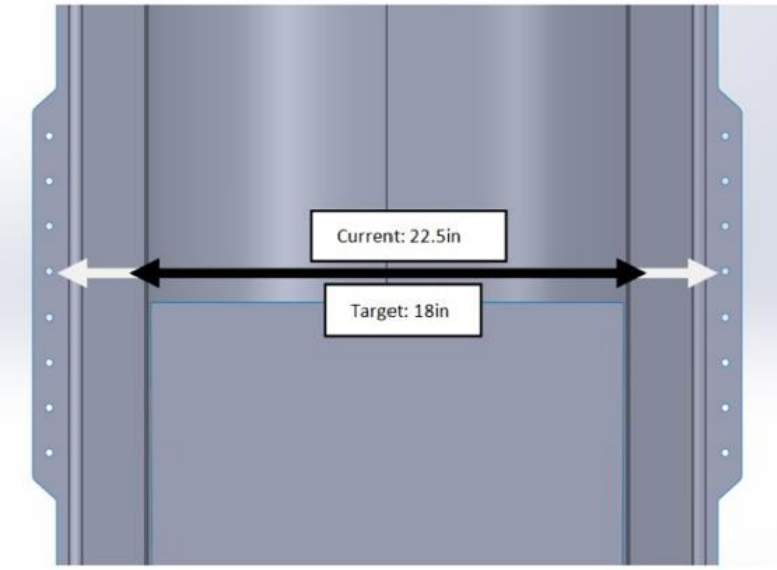

Figure 2. Rigger rails current v. target. Source: Capstone Quad Outline. See reference documentation.

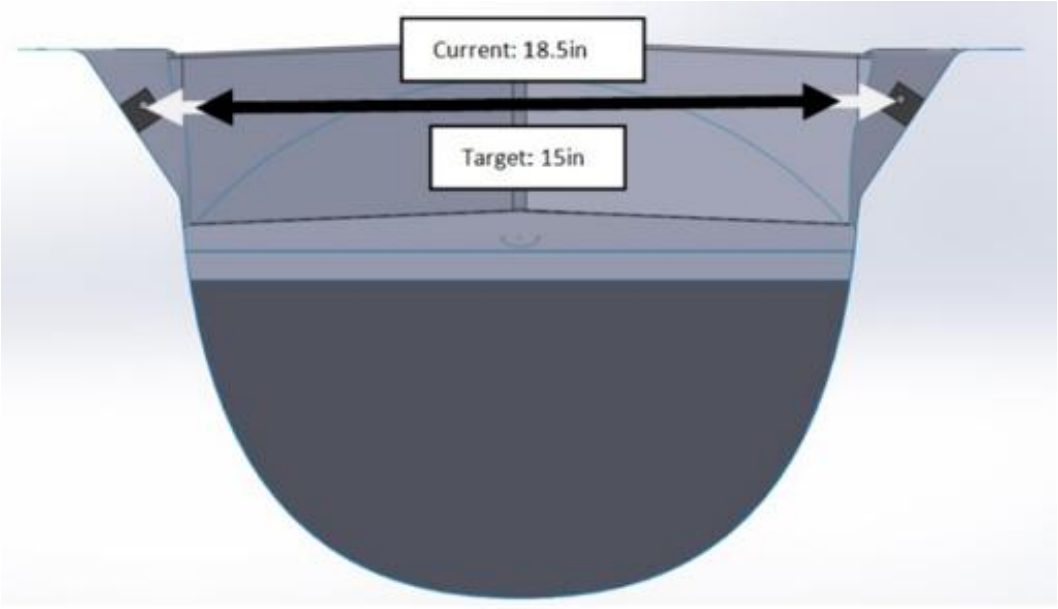

Figure 3. Sweep rails current vs. target. Source: Capstone Quad Outline. See reference documentation.

1.2 Design Requirements and Constraints

The improved racing rowboat design must meet rigorous functional, physical, and environmental requirements to ensure optimal performance and longevity in competitive settings. Structurally, the boat will continue to be manufactured from high-modulus carbon fiber, vacuum-sealed, and resin infused with epoxy. These materials and manufacturing techniques maximize strength while minimizing weight. Given this manufacturing approach, the redesigned hull must remain removable from the molds, thus the design cannot include negative draft angles. Additionally, dimensional modifications to the hull sides will enable compatibility with both sculling and sweep riggers, with the goal of making double

riggers interchangeable on the quad boat. This interchangeability simplifies equipment logistics, as the updated design will bring the gunnel dimensions of the quad in line with the narrower requirements of double boats, allowing both quad and double boats to use the same riggers (see **Error! Reference source not found.** and **Error! Reference source not found.**).

One of the main design goals is to achieve a 20% increase in torsional and lateral stiffness to improve energy transfer from the rower to the water, reducing energy loss by the deflection of the gunnel and flange area. This increase will be accomplished by refining the carbon fiber layup pattern and adjusting the geometry of the gunnel and flange areas (see Figure 4). FEA was used to optimize this new layup, balancing the requirements for stiffness and minimal weight. In addition, updates to the quad structure will focus on reducing lateral deflection while preserving the boat's overall length and key geometry, ensuring consistent handling and stability. The hull will remain the same length, maintaining familiar performance characteristics for rowers and compatibility with existing training setups.

The boat's weight must be kept as light as possible while still meeting stiffness goals. The current design weights are just under the minimum standards: 50 kg for 4x boats and 52 kg for quad sculling boats. Thus, any modifications must prioritize stiffness without significantly increasing weight, maintaining competitive compliance with these weight standards.

Environmental conditions impose additional constraints, as the boat will be exposed to water, sun, and temperature variations. The composite material and epoxy resin will be designed to withstand prolonged exposure to UV light and resist corrosion to achieve a 15-to-20-year lifespan, as specified by Fluidesign. The materials must also allow for easy repair to extend the boat's usability and durability throughout years of races, transportation, and storage. Finally, the boat must perform reliably in water temperatures ranging from 0° to 40°C, ensuring adaptability across a range of climates. This robust combination of functional, physical, and environmental requirements aims to produce a high-performance racing rowboat that meets the demanding standards of competitive rowing while offering resilience in diverse conditions.

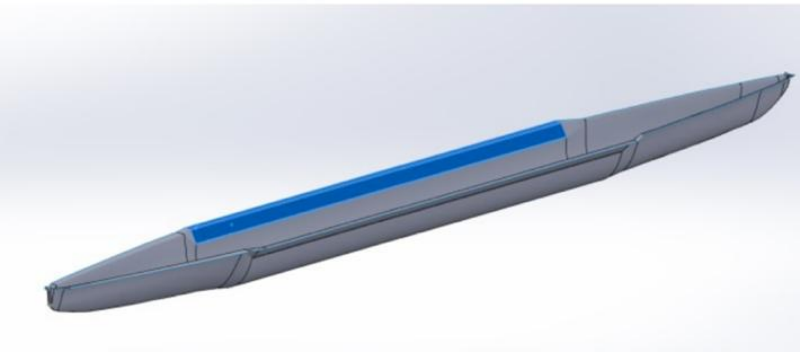

Figure 4. Gunnel/flange area. Source: Capstone Quad Outline. See reference documentation.

1.3 State-of-the-Art and Emerging Technologies

High-performance racing row boats are primarily constructed using carbon fiber because of its superior strength-to-weight ratio. The carbon fiber epoxy process begins by layering carbon fiber fabric into a mold, typically in a weave that ensures strength in multiple directions (see Figure 5) [1].

Epoxy resin is then applied to the fabric using a vacuum seal, which binds the carbon fibers together, using an oven to cure it into a stiff and durable composite material (see Figure 6 and Figure 7). This resin also provides a smooth, hydrodynamic surface. To maximize strength and minimize weight, vacuum bagging is often used to remove excess resin, and the composite is cured under heat to harden the material fully. There are typically three to four pieces that make up the structure of the boat which are then assembled (see Figure 8). This process is used to create all of Fluidesign's boats (see Figure 9). This process creates a lightweight yet extremely strong hull, which is required for optimal speed during races.

Beyond the basic single layer hulls, one of the most popular stiffening methods is the use of a honeycomb core design, sandwiched between two layers of thin carbon fiber [2]. This honeycomb core significantly increases the rigidity of the hull without adding too much weight (see Figure 10). The hexagonal cells in the honeycomb structure provide enhanced support while allowing the material to remain light, making it ideal for competitive boats that require both stiffness and minimal weight. This is the design used for most international and Olympic races.

Another design technique observed by the customers in competition is the addition of a second layer of carbon fiber fabric directly onto the hull [3]. This additional layer further increases stiffness, as multiple layers of carbon fiber aligned at varying orientations improve resistance to flex under load. This method, while slightly increasing the boat's weight, can be fine-tuned to offer an optimal balance of stiffness and performance depending on thickness, area and orientation.

For lower-performance or recreational row boats, more traditional stiffening methods are used, such as adding cross support pieces or utilizing an egg-crate assembly within the hull (see Figure 11) [4]. These methods, while not as weight efficient as carbon fiber layering or honeycomb designs, are effective in reducing hull deflection and maintaining structural integrity at a lower cost.

To further enhance torsional stiffness, the engineering techniques used in modern aerospace applications, such as those in airplane wings, can be adapted to rowing shells [5]. Some racing boats have experimented with techniques derived from aircraft wing stiffening, like the implementation of shear webs or spars (see Figure 12). Shear webs, often constructed from carbon fiber, are placed between two skins (or layers) in a similar fashion to the honeycomb core design but with a different focus. These webs or spars act as reinforcement to counteract torsional twisting forces, distributing the load along the length of the boat and preventing flex. This approach not only improves torsional stiffness but also reduces unwanted vibrations that may arise during high-speed rowing. Although slightly heavier, the trade-off can be beneficial for specific types of competitive rowing that demand enhanced stability. Such advancements borrowed from aerospace design offer promising avenues to achieve highly stiff, optimized hulls suitable for top-tier racing performance.

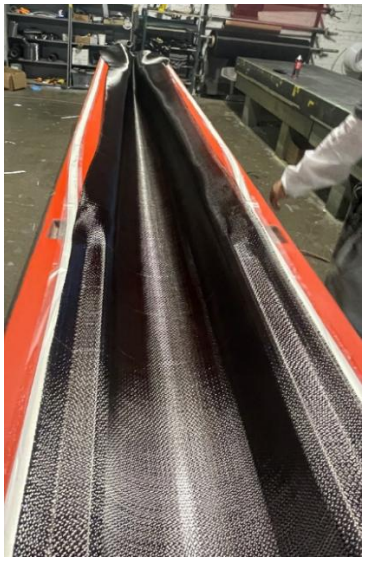

Figure 5. Carbon fiber weave laid into mold.

Figure 6. Oven for vacuum seal epoxy curing.

Figure 7. Hull after vacuum seal molding.

Figure 8. Mold pieces being assembled.

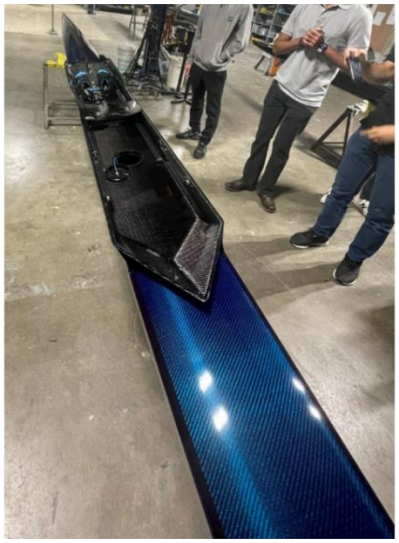

Figure 9. Finished rowboat without riggers.

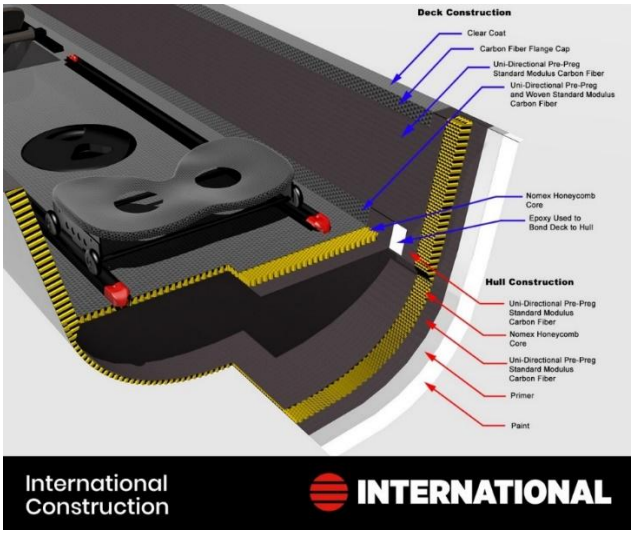

Figure 10. Honeycomb shell design. Source: Wintech racing full core hull build. *https://www.wintechracing.com/technology/hull-construction/*

Figure 11. Rowboat cross-supports - egg-crate assembly. Source: World rowing *https://worldrowing.com*

Figure 12. Shear webs in aircraft. Source: Airfield Models *https://www.google.ca/imgres?q=shear%20webs%20in%20airplane%20wings&imgurl=https%3A%2F%2Fwww.airfieldmodels.com%2Fgallery_of_models%2Frc%2Fwermachts_scorpion%2Fimages%2Fwallpaper%2F17600.jpg&imgrefurl=ht*

1.4 Design Concepts

As stated in *Section 1.1*, the primary goal of this redesign is to improve the lateral and torsional stiffness of the gunnel/flange region of the quad boat. Achieving this objective will improve the performance of the boat by reducing deflection and loss of energy during rowing. However, it is crucial that the final design does not add additional mass to the boat, and it must avoid significant alterations to the current manufacturing process.

Each of the proposed concepts involves some degree of modification to the boat's structure, either in dimensions or material configuration. It is assumed that these concepts will include material alterations aimed at maximizing stiffness, with the final material being a variant of carbon fiber, as determined through FEA. The following concepts have been identified for consideration:

1.4.1 Honeycomb Reinforcements

The honeycomb concept involves the incorporation of a lightweight honeycomb structure, composed of an aramid fiber/phenolic resin honeycomb sandwiched between two sheets of carbon fiber (see Figure 10). This design has the potential for strength to be maximized, with minimal use of material. This concept brings challenges with its cost and would require Fluidesign to modify its current manufacturing process.

1.4.2 Dimensional Changes

For this concept, the dimensions of the gunnel/flange area would be adjusted to match those of Fluidesign's double boat (see Figure 3). By reducing the width and bulkiness of the quad to align with the more streamlined design of the double, the boat's stiffness could be enhanced, and structural weight could be redistributed more efficiently. With the decrease in mass, there is then an opportunity to add layers of carbon fiber to optimize stiffness in the suffering areas. This change would also enable the use

of double riggers on the quad, thereby simplifying production and reducing costs by using a single set of riggers for both boats.

1.4.3 Material Reinforcements

This concept involves the incorporation of additional composite reinforcements to the gunnel or hull of the boat. The placement of these reinforcements will be determined through SolidWorks FEA and additional validation through physical testing in order to determine the weakest points on the boat that would require additional material to enhance the stiffness of the area.

1.5 Selected Concept Development

A Pugh matrix is used to evaluate each concept. The criteria for determining the best solution is decided based on the functional requirements of the boat. The weighting of the design criteria has been determined through the level of importance. Weights of 0.3 being the most valuable, and 0.1 being the least valuable criteria. After evaluating each concept using the matrix, it was deemed that the honeycomb reinforcement concept was not an effective solution due to the manufacturing constraints and the limitations regarding the weight and functionality of the boat. Dimensional changes, along with new carbon fiber layup alterations received equal weights of 2.6, making these concepts the most desirable for the scope of the project. Since these concepts can coexist alongside each other, the selected design concept will include both dimensional changes to accommodate the double riggers, as well as some additional material alterations and reinforcements.

Table 1. Design Pugh Matrix.

Design Criteria	**Relevance**	**Weighting** 0.3 - most importance 0.1 - least importance	**Honeycomb**	**Dimensional Changes**	**Carbon Fiber Layup Alterations**
			3 - fully meets or exceeds the design criteria 2 – adequately meets the design criteria 1 – fails to meet or only partially satisfies the design criteria		
Increases stiffness	Critical for improving the efficiency of power transfer	0.3	**3**	**2**	**3**
Allows for double riggers	Reduces the need for additional manufacturing	0.2	**1**	**3**	**2**
Minimizes weight	Lighter boats improve speed, and rowing efficiency	0.2	**1**	**3**	**2**
Feasible manufacturing	Important for practical implementation	0.2	**1**	**3**	**3**
Maintains key geometry	Essential to avoid unnecessary redesigning and to maintain the proper balance of the boat	0.1	**3**	**2**	**3**
		Weighted Total	**1.8**	**2.6**	**2.6**

1.5.1 Dimensional Changes

To accommodate the double riggers and potentially enhance the boat's stiffness, dimensional adjustments were required, specifically to reduce the width between the gunnels from 572 mm to 457 ~~inches.~~mm. The initial design iteration implemented this change by simply narrowing the distance between the two gunnels, removing any outward bend from the original boat. This iteration can be visualized in Figure 13 and Figure 14. After analyzing this change through FEA, it was found that this alteration weakened the boats lateral stiffness. To fix this issue, the height of the gunnels was shortened from 92 mm to 58 mm which restored a portion of the boat's geometrical stiffness shown in Figure 15 and Figure 16. The length of the full quad boat and the bottom of the hull below the gunnel remain the same as the original model shown in Figure 17.

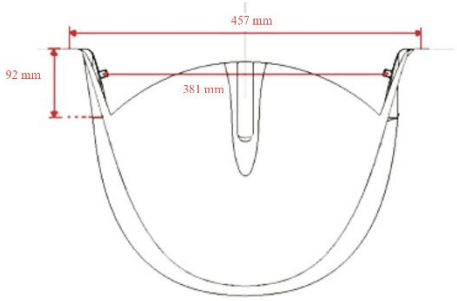

Figure 13. First design iteration dimensions.

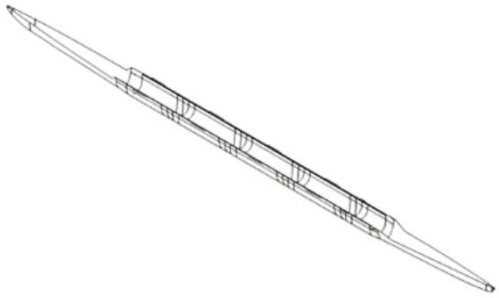

Figure 14. First design iteration full hull.

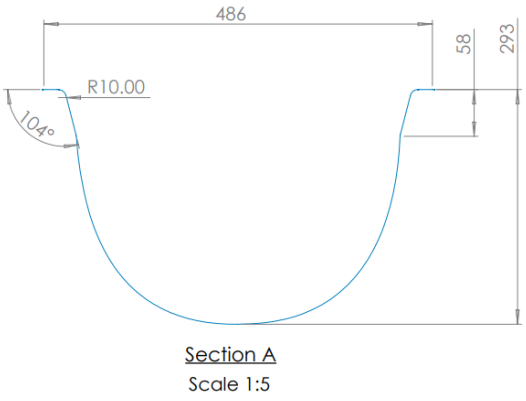

Figure 15. New hull dimensions.

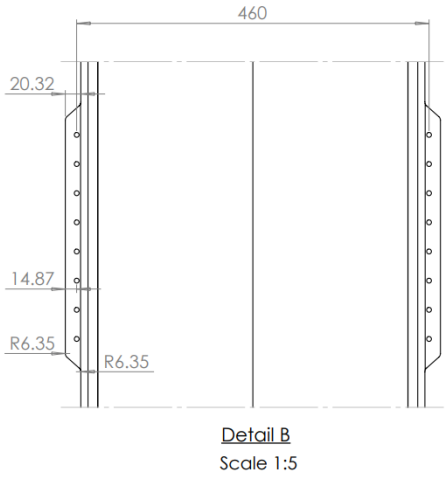

Figure 16. New flange dimensions.

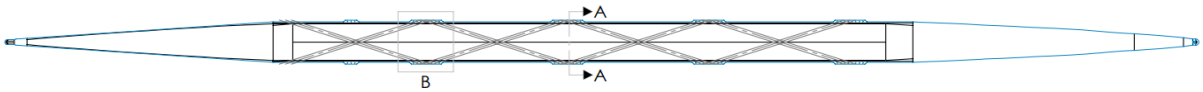

Figure 17. Crossed reinforcement sections

1.5.2 Weight Change

Before selecting materials, a weight calculation of the original hull, and the new dimensional hull designs was performed to estimate how much weight could be reallocated for material reinforcements. The dimensional changes to the hull resulted in a lower area of the gunnel, reducing some of the mass. The updated hull geometry changes also allowed for double riggers to be implemented. These new riggers can also be produced using carbon fiber rather than the current 6061 Aluminum, providing more opportunity for weight to be added via reinforcements as the new riggers are half a pound lighter than the originals.

Original Hull Weight				
Composite	Section of the boat	Area of section (mm^2)	Areal Weight with Epoxy (kg/m^2)	Weight
6 oz twill	Full Hull	9230188	0.33	3.05
12 oz biax	Flange	184894	0.67	0.124
9 oz plain	Flange	184894	0.5	0.0924
9 oz uni	Gunnel	1519098	0.53	0.805
12 oz twill	Full Hull	9230188	0.67	6.18
			Total Weight	10.3 kg

summarizes the weight calculations of the original hull, keeping in mind this calculation only considers the hull of the boat, disregarding the riggers and additional elements within the cockpit of the boat. When compared to the redesigned hull with updated dimensions, the results show a slight 0.2 kg decrease in weight. This weight reduction will be beneficial as it provides flexibility to incorporate additional reinforcements aimed at enhancing the overall stiffness of the hull.

Table 2. Original hull weight.

Original Hull Weight				
Composite	Section of the boat	Area of section (mm^2)	Areal Weight with Epoxy (kg/m^2)	Weight
6 oz twill	Full Hull	9230188	0.33	3.05

12 oz biax	Flange	184894	0.67	0.124
9 oz plain	Flange	184894	0.5	0.0924
9 oz uni	Gunnel	1519098	0.53	0.805
12 oz twill	Full Hull	9230188	0.67	6.18
			Total Weight	10.3 kg

Table 3. Hull weight with dimensional changes.

Hull Weight with Dimensional Changes Only				
Composite	Section of the boat	Area of section (mm^2)	Areal Weight with Epoxy (kg/m^2)	Weight
6 oz twill	Full Hull	9091864	0.33	3.00
12 oz biax	Flange	219214	0.67	0.147
9 oz plain	Flange	219214	0.5	0.109
9 oz uni	Gunnel	1380762	0.53	0.732
12 oz twill	Full Hull	9091864	0.67	6.092
			Total Weight (kg)	10.1

1.5.3 Material Selection

Currently, Fluidesign is using a layup that involves multiple layers of carbon fiber that are arranged longitudinally along the boat. The current layup provided by Fluidesign can be seen in Table 6. The main purpose of this material selection is to determine different carbon fiber composites to be layered to improve the boat's stiffness.

The primary action for this process is to focus back on the design objectives, constraints, and free variables. As stated before, the objectives for the new layup are to increase torsional and lateral stiffness while minimizing mass. The constraints include a fixed length and width, as well as the applicable environmental requirements: it must be UV resistant and durable in fresh and saltwater conditions. The free variable in this application is thickness which will be determined by the number of layers implemented.

Granta is the software used to determine the best epoxy/carbon fiber material configurations. Since the rowers apply forces in multiple directions, Young's modulus, shear modulus, and flexural modulus are the applicable mechanical attributes that were the focus of this material selection. Young's modulus is the measurement of stress over strain. A high Young's modulus indicates high stiffness in tension and/or compression. Shear modulus is used to determine the material with the greatest stiffness against shear stresses caused by the rowers, while high flexural modulus indicates a greater stiffness in bending

applications. Each mechanical property is then used in a material index, which will help to determine how well each material performs in the given application. Since mass is being minimized, the material index will compare each modulus over density.

In Granta, filters are applied to each material property graph to explore the materials that are durable in salt and freshwater conditions, UV radiation, and uses an epoxy resin. As seen in Figure 18 through Figure 19, four Epoxy/carbon fiber materials with various prepregs and layups show the greatest modulus-to-density ratio. These materials are then compared by the material indices, to confirm which material is best in each scenario.

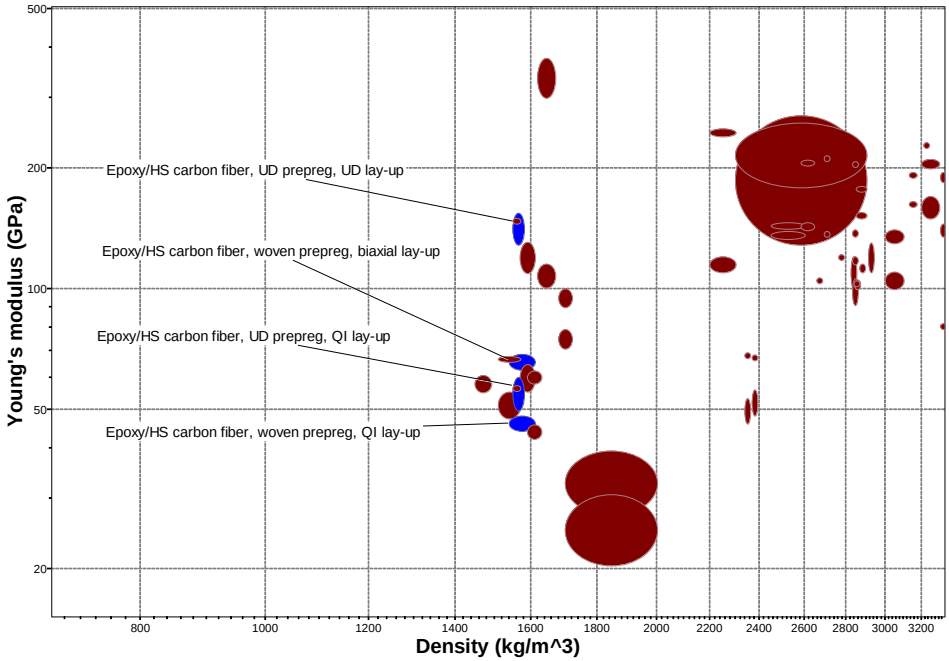

Figure 18. Young's Modulus vs. Density.

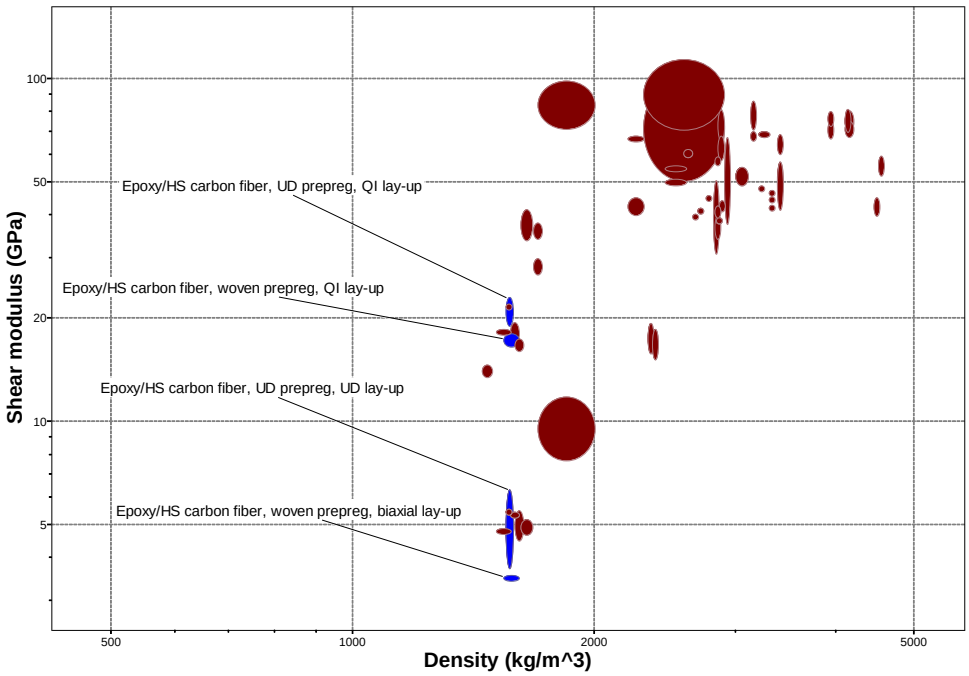

Figure 19. Shear Modulus vs. Density.

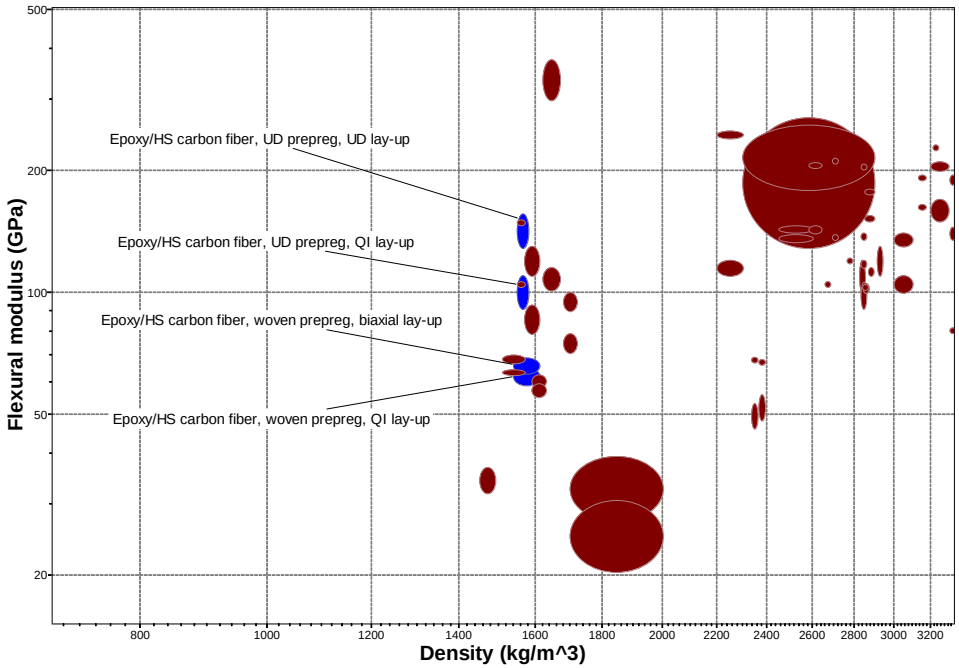

Figure 20. Flexural Modulus vs. Density.

The following table outlines each material's properties and compares each material's indices to determine the best options.

Table 4. Material properties and comparisons.

	Young's Modulus E (Gpa)	Shear Modulus G (Gpa)	Flexural Modulus E_f (Gpa)	Density (kg/m^3)
Epoxy/HS carbon fiber, UD prepreg, QI layup	60.1	23	110	1580
Epoxy/HS carbon fiber, UD prepreg, UD layup	154	6.3	156	1580
Epoxy/HS carbon fiber, woven prepreg, biaxial layup	68.7	3.5	69	1610
Epoxy/HS carbon fiber, woven prepreg, QI layup	48.2	18	65.3	1610

Table 5. Material properties and comparisons over density.

Material indices	E/ρ	G/ρ	Ef/ρ
Epoxy/HS carbon fiber, UD prepreg, QI layup	0.0380	0.0145	0.0696
Epoxy/HS carbon fiber, UD prepreg, UD layup	0.0974	0.00398	0.0987
Epoxy/HS carbon fiber, woven prepreg, biaxial layup	0.0426	0.00217	0.0429
Epoxy/HS carbon fiber, woven prepreg, QI layup	0.0299	0.0112	0.0406

As seen in Table 5, The Epoxy/High Strength (HS) carbon fiber, Unidirectional (UD) prepreg, UD layup are best in unidirectional applications given their high Young's modulus. It is also highly resistant to bending deformation with its high flexural modulus. The Epoxy/HS carbon fiber, UD prepreg, and quasi-isotropic (QI) layup are best for stiffness against shear stresses.

This software was useful in gaining a basic understanding of the performance of carbon fiber, however after analysis of the software, it was found that Granta was only able to account for the most basic weaves of carbon fiber and is not equipped with the vast variety of carbon fiber weaves available on the market. Taking this into account, material research through online suppliers and application through SolidWorks simulation was a large part of the material selection process, aided by physical material testing.

A sample pack of carbon fiber materials containing a sufficient range of weaves and weights was obtained through research and sourced from the producer FibreGlast. Specifications for these materials can be seen in Appendix IV. These specifications were then implemented into SolidWorks FEA to compare with the original materials used by Fluidesign, to identify the optimal materials for

each region of the boat structure, along with a material that could be used for additional reinforcements.

After the materials were imported into SolidWorks and simulated through various tests outlined in *Section 1.5.3*, the following material changes outlined in Table 6 were implemented.

Table 6. Hull Layup Materials.

	Area	Total # of layers	Materials	Total Thickness of area (mm)	Angle from horizontal (degrees)
Original	Full Hull (See Figure 21)	2	3 oz. Twill	0.6	0
			6 oz. Twill		0
	Gunnel (See Figure 22)	3	Biaxial Weave	1.2	0
	Flange (See Figure 23)	4	Unidirectional	1.4	0
New	Full Hull (See Figure 21)	2	3 oz. Twill	0.6	0
			6 oz. Twill		0
	Gunnel (See Figure 22)	3	6 oz. Twill	1.2	0
	Flange (See Figure 23)	4	Unidirectional	1.4	0
	Added Reinforcement Area (See Figure 24)	3	Unidirectional	0.8	20

Figure 21. Full hull.

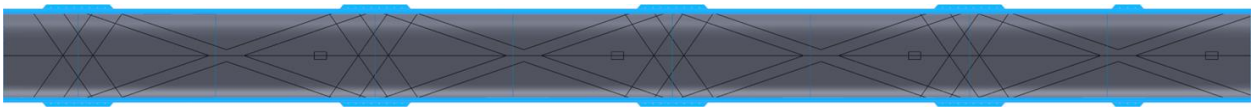

Figure 22. Gunnel area.

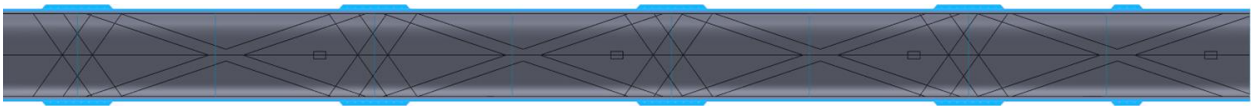

Figure 23. Flange area.

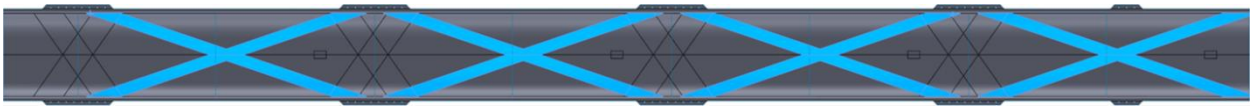

Figure 24. Cross pattern reinforcement.

The changes to the flange area included replacing the 12 oz. biaxial weave carbon fiber, to the 6 oz. twill weave carbon fiber. This change was implemented because it proved to be stronger through SolidWorks analysis without adding any additional weight. Also in the flange area, the 9 oz. plain weave was replaced with the 9 oz. unidirectional carbon fiber which was determined through FEA displacement vectors that proved the unidirectional fabric to be beneficial. 12 oz. twill replaced the 4 oz. biaxial weave in the flange area as well. This increase in weight was allowed due to the lighter weight of the new hull dimensions. Lastly, the implementation of the added reinforcement in the cross pattern along the hull was determined through FEA which displayed the areas and directions that required the most reinforcements.

All material changes described above were incorporated into a final assessment of the updated hull weight in Table 7. When comparing the total weights from Table 3, the total weight of the revised hull reflects an increase of about 0.5 kg from the original design. This slight increase in weight is not considered problematic, as it is offset by weight reductions in other components of the boat, most notably through the implementation of the lighter double riggers which decrease the boat's weight by approximately 0.9 kg, making the end product lighter than the original design.

Table 7. New hull weight.

New Hull with Dimensional and Material Changes				
Composite	Section of the boat	Area of section (mm^2)	Areal Weight with Epoxy (kg/m^2)	Weight (kg)
6 oz twill	Full Hull	9091864	0.33	3.00
6 oz twill	Flange	219214	0.33	0.0720
9 oz uni	Flange	219214	0.53	0.116
9 oz uni	Gunnel	1380762	0.53	0.732
12 oz twill	Full Hull	9091864	0.67	6.09
12 oz twill	Flange	219214	0.67	0.147
22 oz uni	Added Reinforcement Area	767368	0.75	0.576
			Total Weight	10.6 kg

1.6 Cost Analysis

1.6.1 Fluidesign Production Costs

Examining the material costs for the new design outlined in Table 8, the material costs per boat increases to approximately $650 CAD. While this is a high price increase, other design parameters are restrictive. No weight addition with limited dimensional changes meant the design needed high-performance materials as outlined in *Section 1.5.3*. The highest cost increase is due to the material change from the biaxial being replaced by another twill layer.

The investment cost for the new molds to change the boat dimensions will be a large initial investment, with molds of this size costing more than $20k. This is a large upfront cost, but it will be a one-time investment that will enhance the boat's performance and create larger sale opportunities breaching higher-level markets for the quad boats.

The new design incorporates riggers from the double boats. This will simplify the manufacturing process for Fluidesigns boats eliminating the quad riggers from the production. This will save Fluidesign manufacturing time and costs for the aluminum riggers.

Table 8. Material costs.

Component	**Cost Per Unit (CAD)**	**Original Design**		**New Design**	
		Amount (yd)	Cost (CAD)	Amount (yd)	Cost (CAD)
3K Twill	67.39 $/yd	5.5	$370	5.5	$370
Biaxial	48.57 $/yd	2.3	$112	N/A	N/A
Plain	68.82 $/yd	2.3	$158	N/A	N/A
6K Twill	100.4 $/yd	5.5	$552	7.8	$783
Unidirectional	63.08 $/yd	N/A	N/A	11	$694
Material Total		**$1,192**		**$1,847**	
New Molds		N/A		$20,000	
Total		$1,192		$21,847	

1.6.2 Project Costs

The project costs remained under $150, well below the $800 budget shown in Table 9. These costs all went towards material and vibration testing. The first three items in the table were redundant – the piezoelectric sensors, the Arduino kit, and the 22-gauge wire. These items were purchased to build an accelerometer to complete the vibration testing. However, the Arduino vibration test was replaced by the Bluetooth accelerometer. Avoiding these costs would have halved the project costs. Overall, the budget limit posed no issue to the project trajectory.

Table 9. Project costs.

Component	Cost Per Unit [CAD $]	Units	Total Cost [CAD $]
Piezoelectric Accelerometer	20.99	1	20.99
Arduino Kit	23.99	1	23.99
22 Gauge Shielded Wire	15.99	1	15.99
Beeswax	10.49	1	10.49
Bluetooth Accelerometer	53	1	53
Carbon Fiber Sample Pack	19.95	1	19.95
	Total [CAD $]		**144.41**

1.7 Physical Testing & Results

1.7.1 Purpose

Two types of tests were conducted to evaluate the stiffness characteristics of the hull. First, a series of vibrational tests were performed to identify structural weak points along the hull and determine its resonant frequencies, providing insight into the boat's dynamic behavior. Second, a comparative material test was performed to assess the material properties of the carbon weave used within the hull.

The natural frequencies will be obtained through the series of physical vibration tests. These frequencies provide insight on the characteristic vibration modes of the boat structure, while the corresponding mode shapes illustrate how different regions of the hull deform and deflect at those frequencies. Understanding these dynamic properties is vital to avoid resonance, which can occur if the operational frequencies of onboard components align with the natural frequencies. Additionally, the vibration analysis will highlight both local and global stiffness variations throughout the hull. Regions exhibiting high frequency response indicate areas of lower stiffness and must be prioritized when considering reinforcements.

1.7.2 Procedures

1.7.2.1. Vibration Testing Methodology

1. Determine an even number of locations to measure vibrational data along the boat. In this specific project, measuring points on the outside of the hull were prioritized; however, measuring data from inside the boat would also yield valuable information in future analysis.

2. Create an apparatus that allows a repeatable, consistent, force to be applied to the boat in a precise location. For example, a mallet mounted on a nail or rod, allowed to swing freely on its axis supported by a height-adjustable structure, enabling the impact zone to be raised to a specified height (Figure 54 from Appendix I).

3. A thin layer of beeswax can be used to temporarily adhere the light-weight accelerometer to the boat without damping any vibrations. Ensure that points along the entire length of the boat are taken, as well as at varying heights to gather comprehensive comparative data.

   Choosing impact location is dependent on which characteristic is looking to be improved shown below in Table 10:

   Table 10. Characteristics being analyzed for each region of the boat.

Region of the boat	**Characteristics being analyzed**
Bow and Stern	Impact resistance
Midsection (keel area)	Local stiffness and longitudinal load distributions
Below seats and in footwell	Load transfer an mount flexure
Gunwales	Torsional stiffness
Rigger mounting points	Mount deflection and shear resistance

4. When ready to test, place sensor in desired position and prepare impact device. To ensure reliable, repeatable, and meaningful results, test each location at least 3 times and average the data values.

5. For precise analysis procedure, follow detailed guide outlined in Appendix I.

1.7.2.2 Material Testing Methodology

The three-point bend test was appropriate for this application.

1. Prepare carbon samples of single sheets infused with resin that align with ASTM D790-17 standards. With a minimum length of 8.5 cm (ensure every sample has the exact same dimensions). Additionally, sample preparation must be done with utmost care to detail as any dust or frayed edges on the samples during the infusion stage will have adverse effects on the results

2. Following Procedure B in a Type I test (Appendix I) will yield the best results for complex carbon composites. As each sample can only be tested once, it is beneficial to prepare multiple identical samples of each material (at least five) to average data values.

3. Once testing is complete, export time, force, and deflection data to Excel and generate graphs to directly compare the force vs displacement of each sample. Additionally, Equation (10), shown in *Section 1.8.4.2* can be used to compare the stiffness of each sample over time. This data is vital to experimentally compare stiffness values of infused carbon fiber as online data values are not always accurate and often do not include resin.

1.7.3 Process Update

All three rounds of testing conducted throughout the project were originally processed and analyzed using MATLAB. Between Design Day and the Final Report, the team consolidated and translated nearly all analytical components into a unified Python script. This transition was aimed at providing the client with a more accessible, modular, and automated tool for future use. The Python script not only replicates the original MATLAB capabilities but introduces several enhanced features. These include automated file parsing and column matching for varying data formats, resultant acceleration calculation across all axes, peak frequency extraction, and stiffness score computation based on inverse amplitude. Furthermore, the script generates comprehensive visual outputs, such as axis-specific FFT plots, high-resolution 3D spectrograms, and a stiffness heat map with normalized color scaling. It also compiles a structured Excel sheet summarizing all key frequency and amplitude data across test points. By packaging all analyses into a single streamlined tool, Fluidesign is empowered to perform advanced structural and vibrational diagnostics with minimal setup and a higher degree of analytical depth than was previously possible using MATLAB alone.

1.7.4 Data Analysis: Python Stiffness Tool

This Python program performs a full-spectrum stiffness analysis of an Olympic-class Quad 4X rowing shell using tri-axial accelerometer data collected at multiple locations along the boat. It begins by scanning the working directory for all raw acceleration data, each of which corresponds to a unique sensor measurement point. The data in each file includes acceleration values along the X, Y, and Z axes, recorded over time, as well as other data gathered by the sensor that is irrelevant to this project (Figure 59 of Appendix III). The script first parses and sanitizes this data, ensuring proper numerical formatting and handling of any missing or invalid values. Then it averages the data for every measurement at each location and automatically determines the time step, which establishes the sampling rate necessary for frequency analysis. Each axis's signal, along with the computed resultant acceleration vector (the Euclidean norm of the X, Y, Z components), is then processed using a Fast Fourier Transform (FFT) to convert the data from the time domain into the frequency domain (Figure 25).

To improve signal clarity and reduce spectral leakage, a windowing function is applied prior to the FFT execution. From the FFT output, the program extracts peak amplitudes and corresponding frequencies for each axis, skipping the 0 Hz component to avoid DC bias. These peaks are used to identify the highest and lowest harmonic frequencies in the structure, excluding the resultant axis to avoid redundancy. A stiffness score is then computed as the inverse of the peak resultant amplitude, providing a unitless measure of structural compliance. Lower amplitudes (and thus higher scores) indicate stiffer

regions with reduced vibrational response, while higher amplitudes imply flexibility or potential structural weak points.

The results for each test point, including peak frequencies, amplitudes, harmonic extremes, and stiffness score, are stored in a well-formatted Excel spreadsheet for documentation and comparative study. In parallel, the program generates frequency response plots for all axes, and a 3D spectrogram for the resultant vector that visualizes how deflection and strain energy vary over time (Figure 26). These spectrograms are displayed with deflection on the Z-axis and strain energy on the Y-axis, providing intuitive insights into the temporal dynamics of hull response. Each visual is exported as an image for archival or presentation use.

Finally, the program aggregates all stiffness scores into a heatmap over a scaled boat diagram (Figure 27) marking each sensor location with a color-coded indicator (ranging from red for low stiffness to green for high). An accompanying color-coded sensor location legend is also generated (Figure 60 of Appendix III). This offers a spatial visualization of reinforcement or material reconfiguration. The entire process is executed automatically and consistently across all sensor points, enabling engineers to rapidly assess stiffness distributions, evaluate design changes, and iteratively optimize the hull structure. This tool supports data-informed decision-making in high-performance boat development by translating raw accelerometer data into actionable insights on material performance, modal behavior, and structural integrity. (Stiffness_Analysis.py is currently in alpha testing and only supports the generation of heat maps in a straight line, if data is taken at varying heights, update code or interpolate visual data)

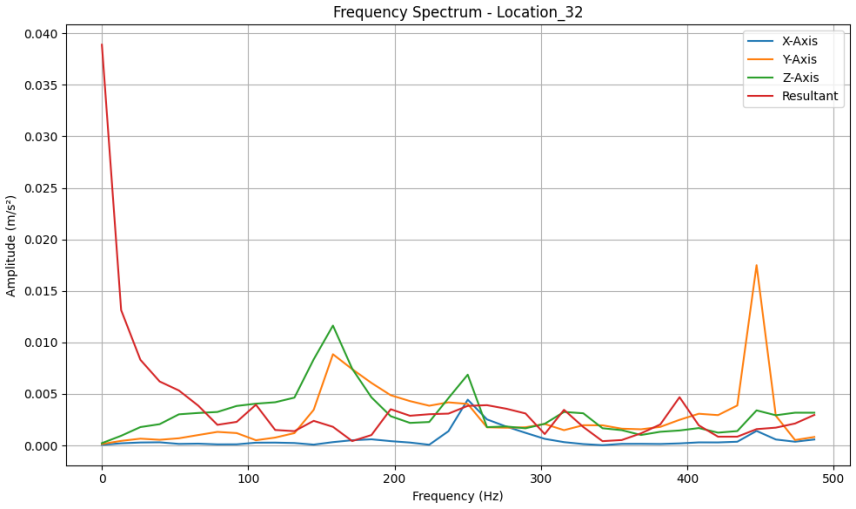

Figure 25. Comprehensive Frequency Spectrum.

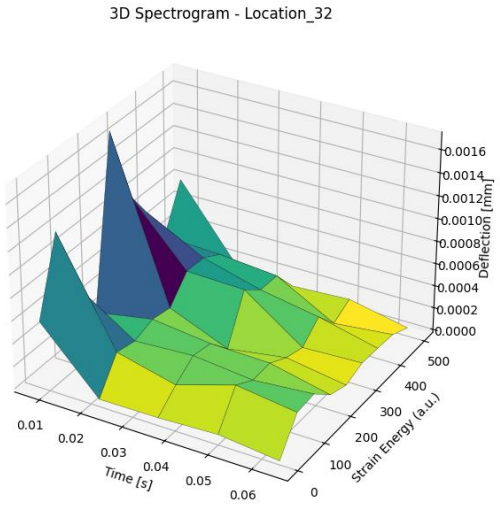

Figure 26. 3D Spectrogram.

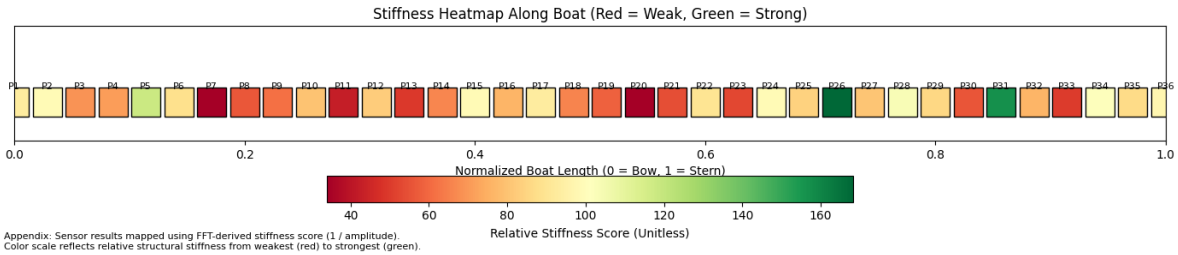

Figure 27. Heat map for designated measurement locations.

1.7.5 Testing Results

1.7.5.1. Test 1

The initial test was conducted to establish a baseline for the simulations. A known force was applied to the boat (~200 N), and vibrational data was collected at various points along its structure. This data allowed for the identification of structural weak points exhibiting excessive deflection. The boat was supported on two padded stands, with a total of 36 measurement points recorded. Deflection was measured along the X, Y, and Z axes.

To process the collected data, a Hanning window was applied in MATLAB to smooth the signals, followed by a Fast Fourier Transform (FFT). This enabled the extraction of frequency-domain magnitudes. The data were subsequently exported to Excel, where a heat map was generated to visualize areas of the boat with the highest frequencies, indicating regions of maximum deflection under load.

Based on the results, high deflection and resonance can be seen primarily in the midsection of the hull. The data follows a wave trend that ripples from the highest zone between rigger 2 and 3

and roughly 150 mm from the upper lip of the gunnel. This wave amplitude dips between each rigger and increases again as it moves closer to the next rigger. Riggers 1 and 4 displayed the highest stiffness values with lower resonance. The outer edges of the boat, beginning 170 mm horizontally from each end rigger, display strong torsional and lateral stiffness. Testing below 12 inches from the upper edge of the gunnel was not taken, which is recommended for Test #2.

The original plan was to carry out this testing using a custom-built accelerometer constructed using 5, 3.5V analog piezoelectric sensors, and an Arduino Uno (Figure 28). This setup encountered multiple challenges, including sensitivity calibration issues, inconsistent signal output, electrical noise interference, and difficulties in achieving reliable data acquisition. As a result, the team opted, just one week before the scheduled test date, to replace the custom system with a single, commercially available, Witmotion Bluetooth tri-axial accelerometer (Figure 29). This solution met all project requirements and functioned with minimal complications, allowing the test to proceed smoothly.

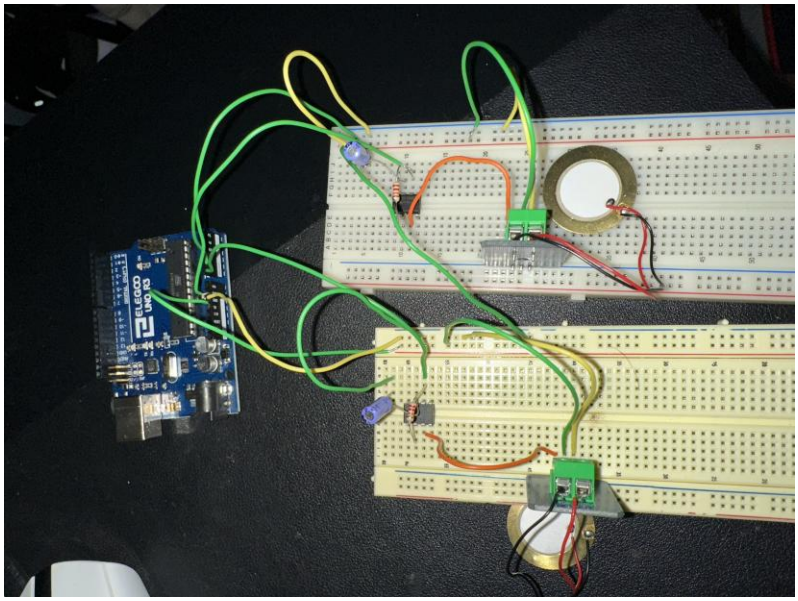

Figure 28. Initial accelerometer setup.

Figure 29. Bluetooth accelerometer.

1.7.5.2 Test 2

The second test was conducted to verify the accuracy of the first test and to refine the results obtained from the heat map. In this test, the boat was suspended from the ceiling using two boat straps, which were positioned near the outer edges of the boat. The impact applied was the same as in the first test, with the only variation being the locations of the sensors Figure 30). A total of 20 different measurement points were used to collect vibrational data. The impact point was centered on the boat to minimize swaying, which could otherwise distort the results.

For data processing, the frequency-domain was windowed to include only the maximum deflection occurring after the impact, as well as the initial resonance. This was done to exclude the effects of the boat's overall movement following the application of force, which would otherwise skew the analysis. The heat map generated from this test showed a high degree of alignment with the results from the first test, as well as with the predictions from the Finite Element Analysis. The data from both tests were combined to create a comprehensive heat map (Figure 31).

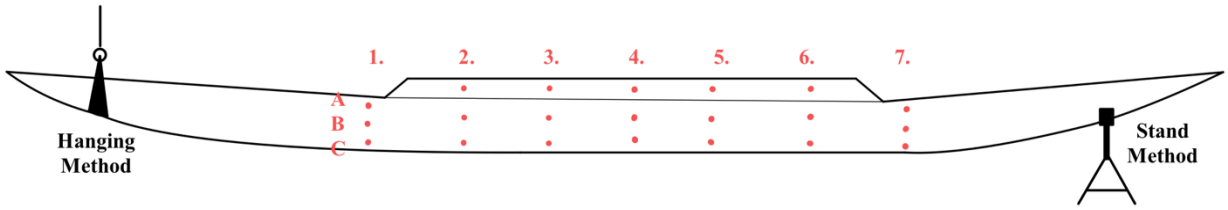

Figure 30. Reading locations.

The results provided a wider look at global stiffness with a larger area of measure. Taking fewer data points was intentional as the midsection was thoroughly mapped in Test #1. The increased accuracy of data, as a result of suspending the vessel, allowed for finite processing of resonance throughout the weak zones to determine the best methodology for stiffening. The cross-pattern fiber strips were unanimously decided as the most feasible option with the best results. Due to the nature of the wave pattern generated by the gaps between the riggers, eight unidirectional strips of carbon fiber tensioned at angles indicated in Figure 30 would provide the greatest support.

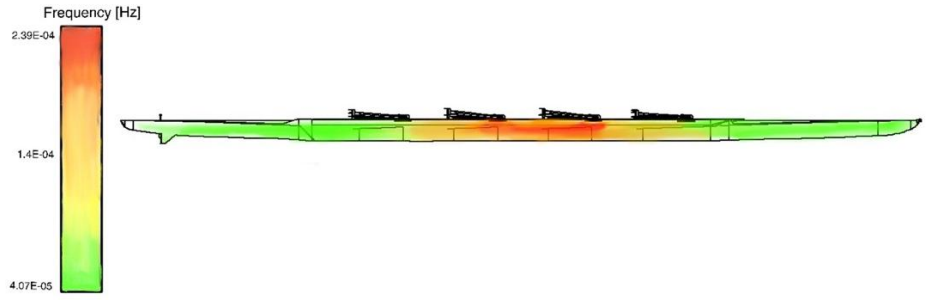

Figure 31. Experimental Heat Map.

1.7.5.3 Material Test

The results of the three-point bend test, as depicted in the force versus displacement graph (Figure 32), demonstrates distinct mechanical behaviors across various carbon fiber weaves. Among the tested configurations, the 9 oz unidirectional weave, 10.9 oz twill, and the 19.8 oz twill specimens exhibited the highest stiffness, as indicated by their steep initial force-displacement slopes and ability to sustain higher loads at increased displacement ranges. These materials also maintained structural integrity throughout the testing process, making them favorable for implementation in the stiffness-critical application. Conversely, the 22.3 oz unidirectional specimen displayed a characteristic brittle fracture mode, evidenced by an abrupt decline in force following peak load with limited plastic deformation. This brittle failure presents a risk of sudden material failure under operational loads, rendering it unsuitable for continued use. Based on these observations, the aforementioned stiffer materials have been selected for further development and integration.

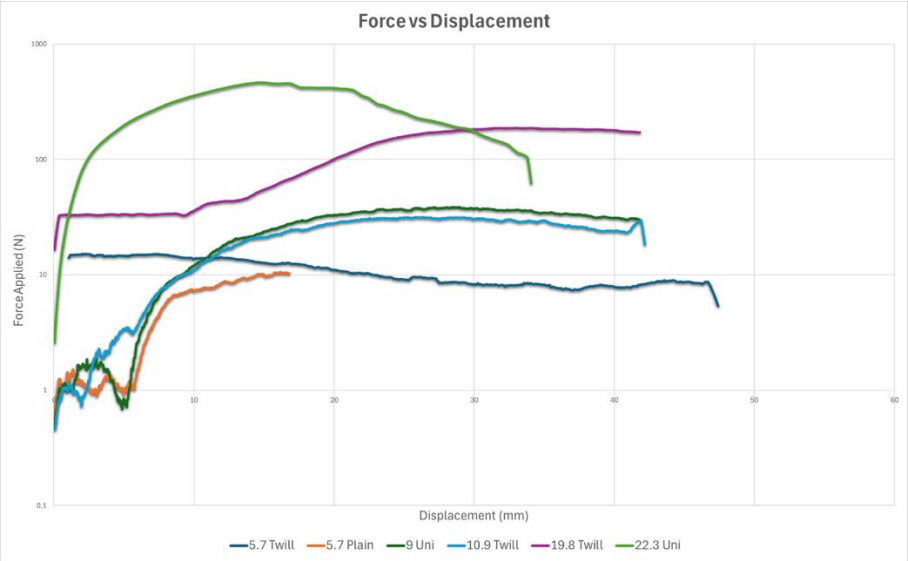

Figure 32. Material test result graph.

1.7.6 Testing Summary

The two experimental tests as well as material testing and simulation provided critical insight into the vibrational behavior and structural weakness of the rowing shell shown in Table 11. The experiments consistently identified the midsection of the hull, particularly beneath the rigger mounts, as an area of concern for excessive deflection under load. Leveraging the additional data processing capabilities introduced through the Python analysis script, the team was able to confirm that the existing biaxial carbon fiber layup performs well in longitudinal stiffness but lacks adequate shear resistance. Considering this, the primary design recommendation is to reinforce the hull using unidirectional carbon fiber strips arranged in a cross-pattern along the length of boat, overlapping on the bottom of the boat. This modification would emulate the benefits of triaxial fiber by enhancing shear strength and improving the distribution of multidirectional loads while minimizing additional weight. Such a reinforcement strategy is

expected to reduce structural deflection in critical zones based on simulation, as well as improve energy transfer during rowing strokes, and ultimately enhance the overall performance and durability of the boat.

Table 11. Test Summary.

Test	Method	Acceptance Criteria	Results
Stiffness Test #1	Boat supported on two padded stands. A known force applied. Vibration data collected at 36 points. FFT and Hanning window applied in MATLAB	Identify baseline structural response. Detect weak points showing excessive deflection via high-frequency vibration response.	Heat map revealed high-frequency response (high deflection) in central hull regions. Weaknesses aligned with the expected stress zones under rigger mounting.
Stiffness Test #2	Boat suspended from ceiling using two straps near outer edges. Same force applied, 20 sensor locations prioritizing higher and lower regions than Test #1. FFT applied to windowed signal excluding post-impact drift in MATLAB.	Validate Test 1 results. Confirm consistent weak points under altered boundary conditions. Eliminate swaying artifacts.	Results aligned with Test 1 and FEA predictions. Central deflection confirmed. Combined data improved spatial resolution of final stiffness heat map.
Material Testing	Conducted 3-point bend test on 10 cm x 6 cm carbon fiber samples with varying weaves and areal weights. Compared deflection, stiffness, and failure loads.	Assess stiffness-to-weight ratio, flexural modulus, and shear response of test laminates. Identify superior reinforcement candidates.	Biaxial samples performed well in longitudinal stiffness but showed poor shear resistance. Unidirectional samples displayed high bending resistance and rigidity.

1.8 Simulation & Results

The following FEA simulations are used to measure the stiffness increase of the proposed solution above. These simulations replicate the forces applied to the boat by the rowers through a rowing stroke to get realistic areas of deflection for the boat's application. All five studies ran – three analyzing row stroke forces, one study examining torsion, and one frequency study – use the material layup outlined in *Section 1.5.3.* All material data inputted to SolidWorks are outlined in Appendix IV. SolidWorks allows for composite materials to be applied to the boat; thus, the boat was divided into the following sections with applied materials, shown in section XXX which creates a more accurate model versus modeling as one uniform material. Both models also included the seats in the hull as they add additional reinforcement to the model.

1.8.1 Mesh Analysis

Ensuring mesh quality reduces the error in the simulation by increasing the accuracy of the mathematical model. The mesh size was reduced until grid independence was reached. Grid independence is achieved once mesh refinements no longer affect the output values of the study. For this project, an acceptance criterion of 2% was used. Further iterations below this criterion would have made each run time over half an hour. Due the the number of simulations that had to be run, this was not feasible. The mesh was refined from 50 mm down to 8 mm per element after five iterations seen in Table 12 and Figure 33. Other mesh elements implemented to ensure mesh quality was a minimum aspect ratio of 1.3 which determines the height versus width of the element, 1 being a perfect ratio and higher numbers being offset. Orthogonality of 10 degrees as a minimum, which determines the angle from the center of one element to the next, zero degrees being perfectly aligned and ninety being the max difference angle. Skewness below 0.3 where a perfect element has all equilateral angles giving it a skewness of zero and a shape like a parallelogram having a high skewness ratio closer to 1. The maximum growth rate was set to 1.3 meaning any element can only be 1.3 times larger than the one beside it. All of these elements ensure the mesh is set up to limit errors in the mathematical model by breaking the model into even small finite sections from which forces can easily transfer from one element to the next seen below in Figure 34. This mesh was used for all five simulations, refinements seen below in Figure 35.

Table 12. Mesh refinement iterations.

Iteration	Grid Size (mm)	Max Displacement (mm)	% Diff
1	50	5.24E-02	
2	25	6.53E-02	32
3	14	7.26E-02	11
4	10	7.51E-02	3
5	8	7.59E-02	1

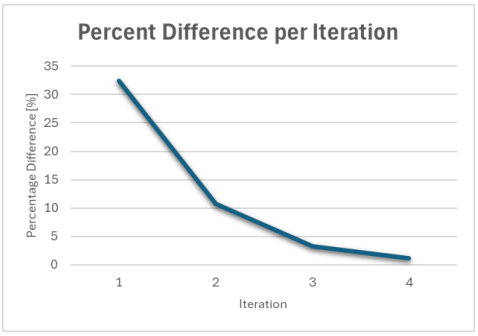

Figure 33: Force change per iteration.

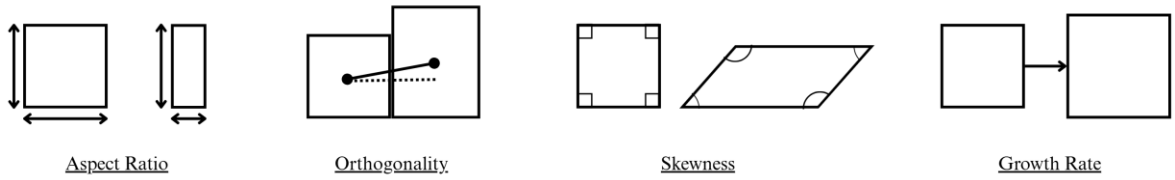

Figure 34. Mesh quality elements.

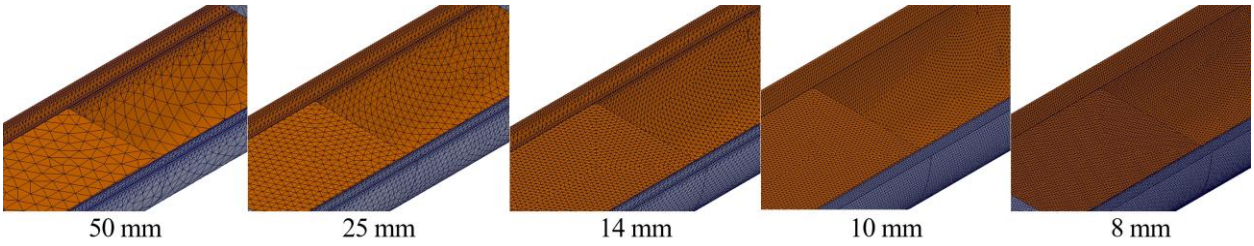

Figure 35. Mesh refinement iterations

1.8.2 Row Stroke Analysis

The simulations were modeled after the forces acting on the boat through a scull row stroke with four rowers. The three points of interest modeled are at the start of the rowing stroke, the point of maximum force, and the end of the rowing stroke. Looking at Figure 36 from a study recording forces through a row stroke of two rowersFigure 1 as a function of position, the points of interest correlate to 100 N at -55 degrees, 650 N at -20 degrees, and 250 N at 10 degrees. These angles are defined with the zero axis perpendicular to the hull shown in Figure 37. Each force was halved as the graph shows results for the sweep rowing and this simulation tested scull rowing. Halving the values accounted for the difference of two oars versus one. The oar was assumed to be acting downwards at a 10-degree angle through these simulations. Equations (1) through (9) calculate the forces in each direction applied to the end faces of the riggers for the simulations.

Start of stroke:

$$F_z = \left(\frac{F}{2}\right) sin\theta = \left(\frac{100}{2}\right) \sin(10) = 8.68\ N \tag{1}$$

$$F_y = F_{xy} sin\emptyset = \left(\left(\frac{F}{2}\right) cos\theta\right) sin\emptyset = \left(\left(\frac{100}{2}\right) \cos(10)\right) \sin(-55) = -40.34\ N \tag{2}$$

$$F_x = F_{xy} cos\emptyset = \left(\left(\frac{F}{2}\right) cos\theta\right) cos\emptyset = \left(\left(\frac{100}{2}\right) \cos(10)\right) \cos(-55) = 28.24\ N \tag{3}$$

Peak of stroke:

$$F_z = \left(\frac{F}{2}\right) sin\theta = \left(\frac{650}{2}\right) \sin(10) = 56.44\ N \tag{4}$$

$$F_y = F_{xy} sin\emptyset = \left(\left(\frac{F}{2}\right) cos\theta\right) sin\emptyset = \left(\left(\frac{650}{2}\right)\cos(10)\right)\sin(-20) = -109.5\ N \quad (5)$$

$$F_x = F_{xy} cos\emptyset = \left(\left(\frac{F}{2}\right) cos\theta\right) cos\emptyset = \left(\left(\frac{650}{2}\right)\cos(10)\right)\cos(-20) = 300.8\ N \quad (6)$$

End of stroke:

$$F_z = \left(\frac{F}{2}\right) sin\theta = \left(\frac{300}{2}\right)\sin(10) = 25.65\ N \quad (7)$$

$$F_y = F_{xy} sin\emptyset = \left(\left(\frac{F}{2}\right) cos\theta\right) sin\emptyset = \left(\left(\frac{300}{2}\right)\cos(10)\right)\sin(10) = 26.05\ N \quad (8)$$

$$F_x = F_{xy} cos\emptyset = \left(\left(\frac{F}{2}\right) cos\theta\right) cos\emptyset = \left(\left(\frac{300}{2}\right)\cos(10)\right)\cos(10) = 145.5\ N \quad (9)$$

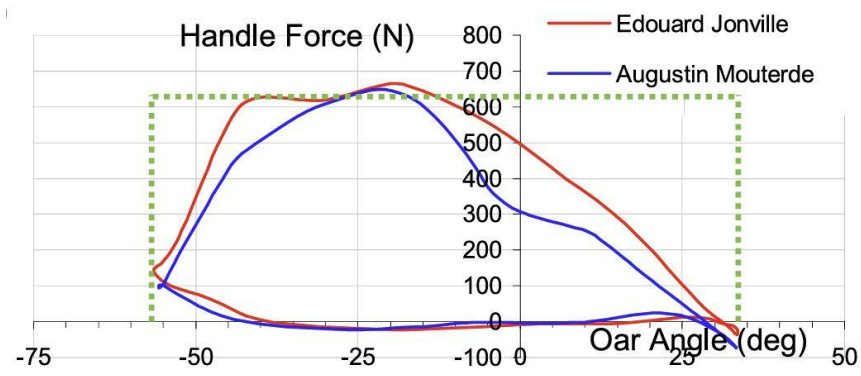

Figure 36. Forces as a function of oar angle. [12]

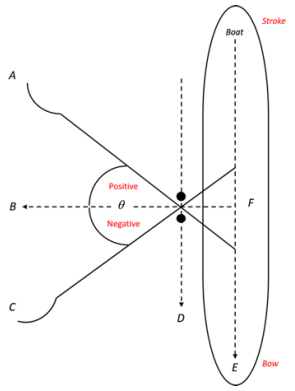

Figure 37. Oar angles. [13]

1.8.3 Simulation 1: Torsional Stiffness Along the Longitudinal Axis

1.8.3.1 Torsional Setup

For this setup, round plates are added to the modified hull to allow bearing fixtures to be placed on their edges seen in Figure 38. End plates for torsion model.. This allows for support without restraining rotation along the longitudinal axis. In sweep rowing, torsion along the longitudinal axis will occur as the downward-acting forces are unbalanced, unlike scull rowing. Only the downward portion of the force from the oar will contribute to this torsion (F_z). This will be a force on 112.9 N acting on alternating riggers. A static study is performed to model the torsion, as static studies have the most material properties and fixtures available. This allows for the materials to be modeled as composites as discussed above.

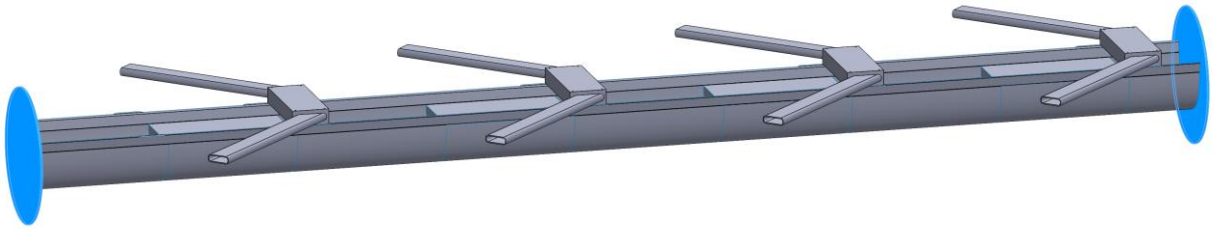

Figure 38. End plates for torsion model.

1.8.3.2 Torsional Results

The simulation results shown in

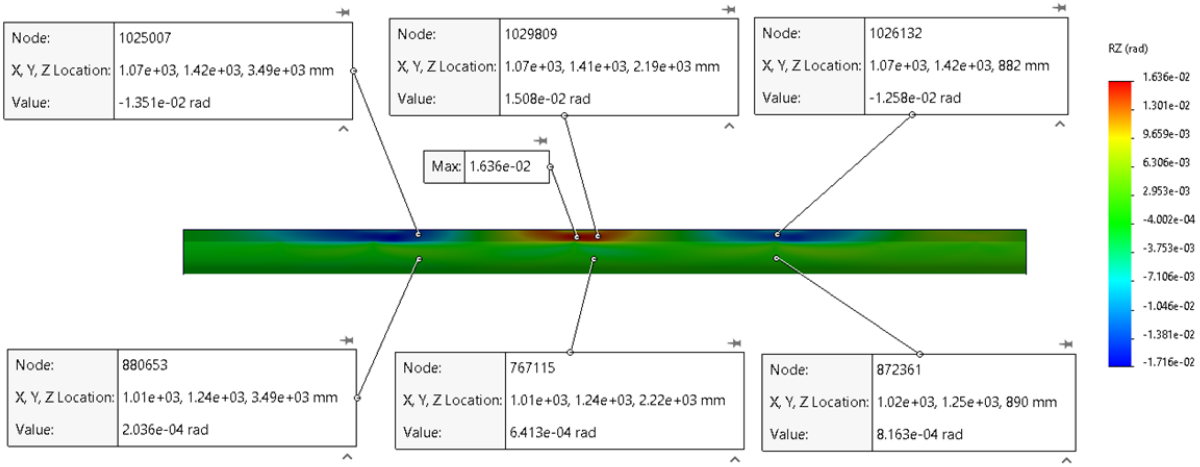

and Figure 40 and calculated in equations (10) through (12) show a stiffness increase of 388% calculated in Equations (10) through (12). The area of max displacement, in the gunnel of the hull below the riggers decreased from 1.64E-02 radians to 3.35E-03 radians. The large decrease in deflection of the torsional model is caused by the reduction of the gunnel height, width, and angle. The overall deflection is further discussed below in section *Section 1.8.6*.

$$Model\ 1: Stiffness_1 = \frac{T}{\theta_o} = \frac{F \times d}{\theta} = \frac{112.9\ N \times\ 0.9\ m}{1.64\ e^{-02}\ rads} = 6.21\ e^{+03}\ \frac{Nm}{rad} \qquad (10)$$

$$Model\ 2: Stiffness_2 = \frac{T}{\theta} = \frac{F \times d}{\theta} = \frac{112.9\ N \times\ 0.9\ m}{3.35\ e^{-03}\ rads} = 3.03\ e^{+04}\ \frac{Nm}{rad} \qquad (11)$$

$$\%\ increase_{1-2} = \frac{Stiffness_2 - Stiffness_1}{|Stiffnes_1|} \times 100$$

$$= \frac{3.03\ e^{+04} - 6.21\ e^{+03}}{|6.21\ e^{+03}|} \times 100 = 388\% \qquad (12)$$

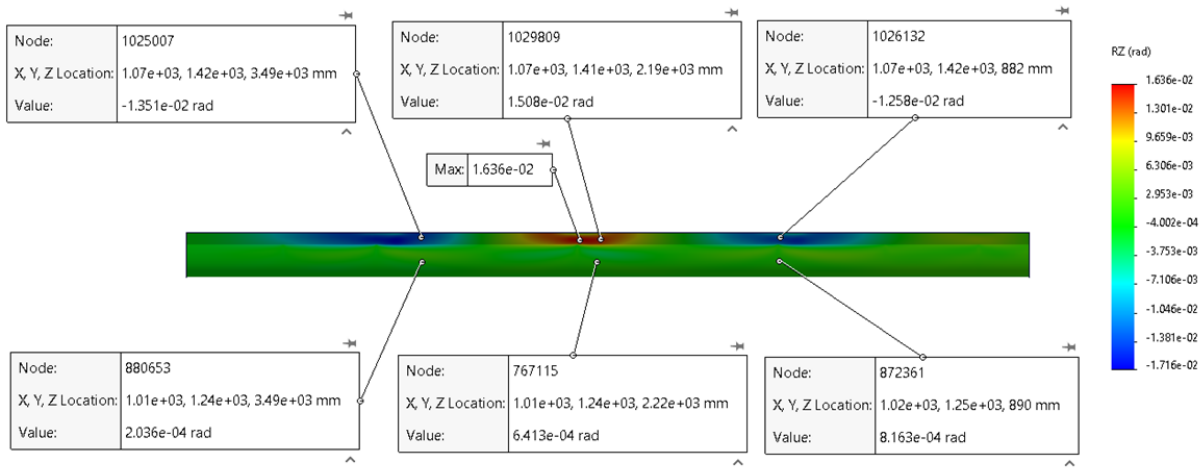

Figure 39. Torsion of original model.

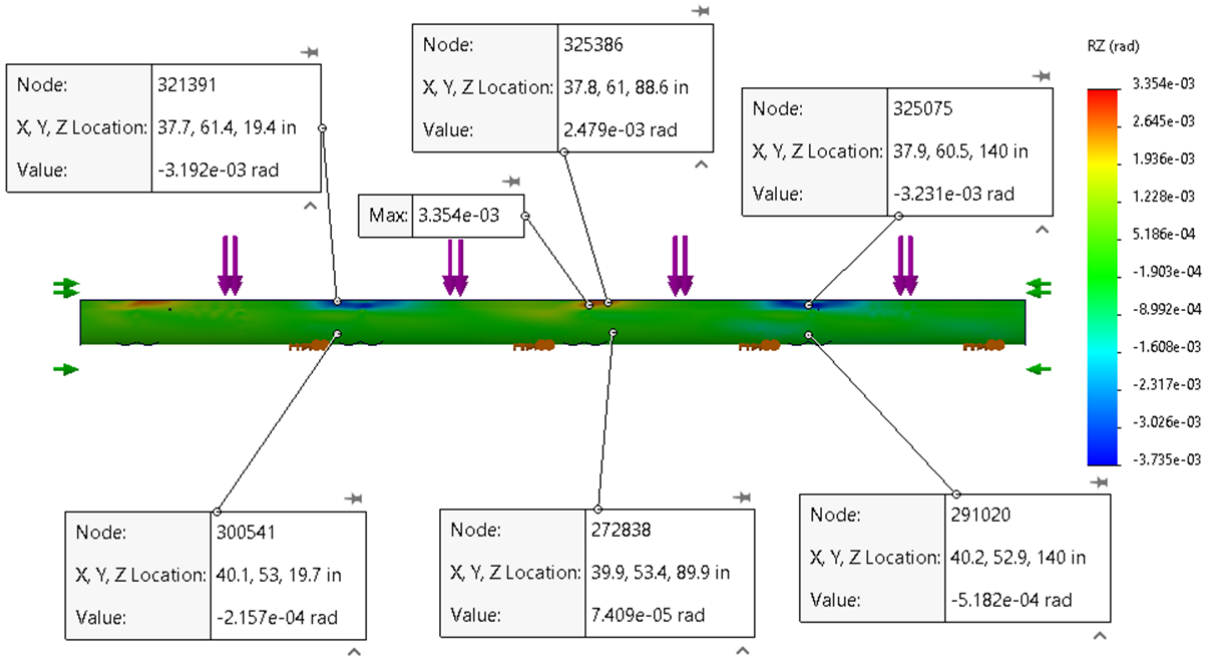

Figure 40. Torsion of the proposed model.

1.8.4 Simulations 2-4: Rowing Simulations

1.8.4.1 Setup

The following three simulations are static studies using composite materials defined in *Section 1.5.3* For this analysis, the three points through the rowing stroke of interest found in *Section 1.8.2* were applied to the end faces of the riggers shown in purple in Figure 41. Immovable fixtures were placed where the footrests lie in the hull shown in green in Figure 41. This is to balance the opposing force the rowers impart where they push through their feet. With this fixture, the forces on the riggers act relative to the

forces from the rowers' legs. Overall, this simulation is difficult to accurately model as there are many moving parts in a rowing stroke as seen in Figure 42. This model omitted the hydrostatic forces from the water as well as the weight of the rowers. The boat model is also reduced by removing the ends as they cause stress concentrations and complicate the analysis. Symmetry fixtures are placed to the ends where the model is reduced to reintroduce strength to the model.

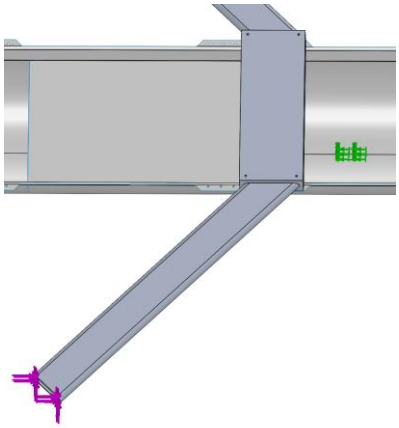

Figure 41. Forces and fixtures for force analysis.

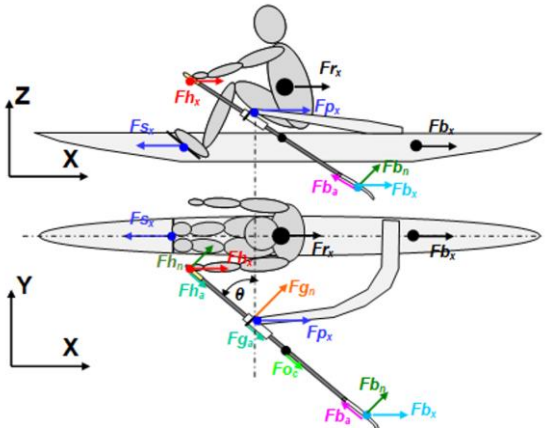

Figure 42. Forces acting through a row stroke.

1.8.4.2 Original Design

The stiffnesses calculated below in Equations (17) through (19) use the forces calculated in Equations (1) through (9) and the maximum deflections seen in the three simulations shown in Figures 43 through 45. The stiffness increase changes brought forward from the new design are outlined in *Section 1.8.4.3*.

Start of stroke:

$$Stiffness_1 = \frac{F}{\Delta x} = \frac{50}{1.549e^{-2}} = 3{,}228\frac{N}{mm} \tag{17}$$

Highest force:

$$Stiffness_1 = \frac{F}{\Delta x} = \frac{325}{9.958e^{-2}} = 3{,}392\frac{N}{mm} \tag{18}$$

End of stroke:

$$Stiffness_1 = \frac{F}{\Delta x} = \frac{150}{4.577e^{-2}} = 3{,}277\frac{N}{mm} \tag{19}$$

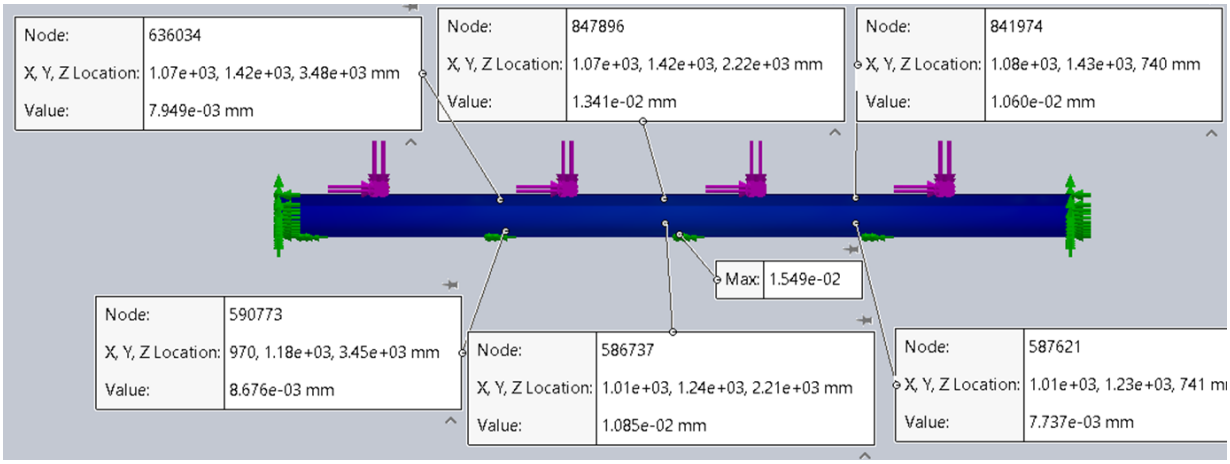

Figure 43. Original model: Start of stroke.

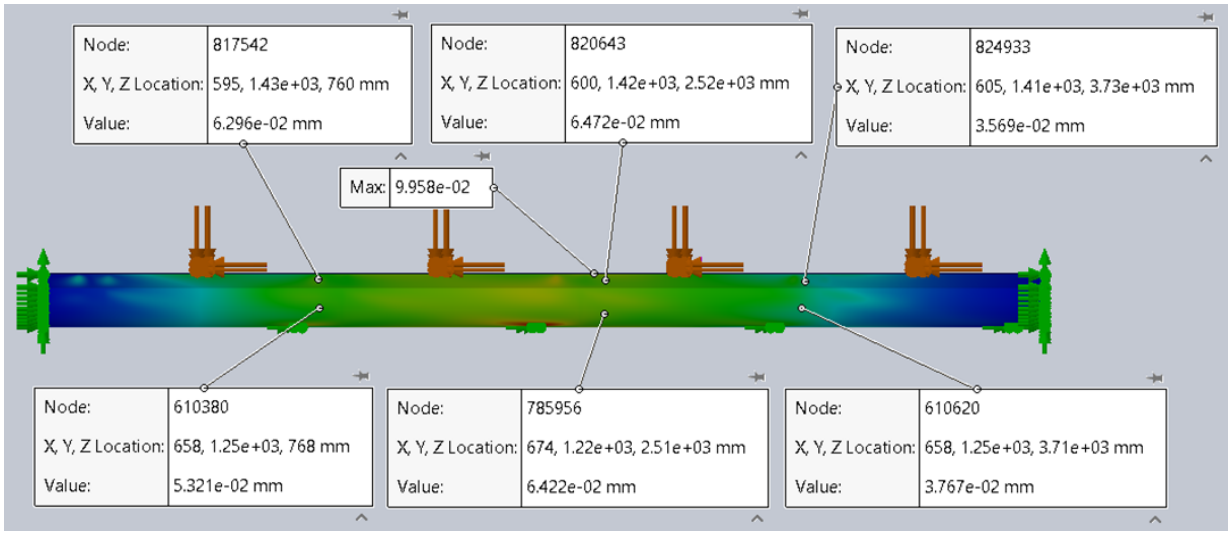

Figure 44. Original model: Top of stroke.

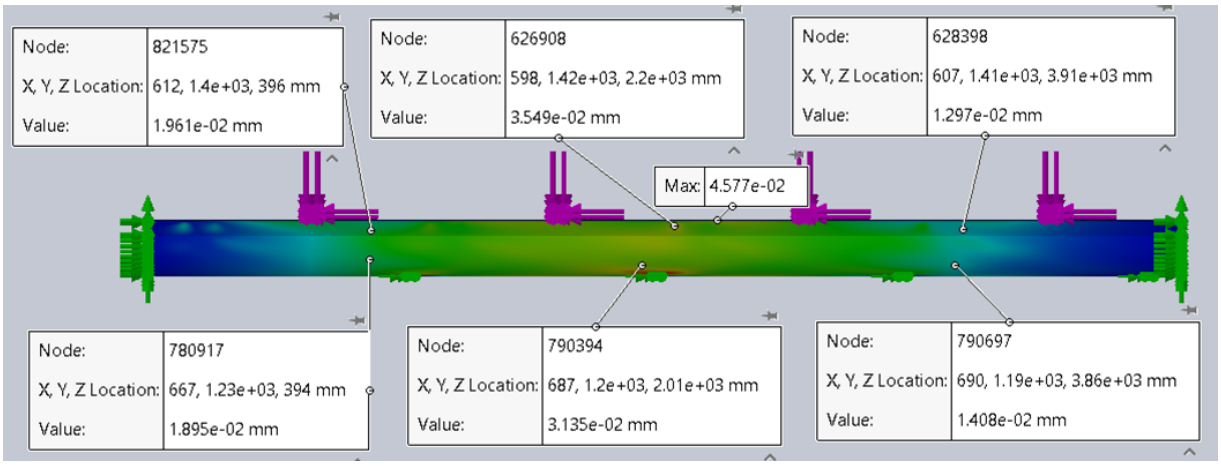

Figure 45. Original model: End of stroke.

1.8.4.3 Proposed Design: Dimensional Changes and Material Addition

The stiffnesses calculated below in Equations (20), (22), and (24) take the forces calculated in Equations (1) through (9) and the maximum deflections seen in the three simulations shown in Figures 46 through 48. The smallest increase in stiffness is at the start of the stroke where it is only of 7% shown in Equation (21). The top of stroke and end of stroke stiffness increases are both above target being a 26% and 38% increase, respectively, shown in Equations (23) and (24). The stiffness increase changes brought forward from the new design are further discussed in *Section 1.8.6.*

Start of stroke:

$$Stiffness_2 = \frac{F}{\Delta x} = \frac{50}{1.448e^{-2}} = 3{,}453\,\frac{N}{mm} \tag{20}$$

$$\%\ increase_{1-2} = \frac{Stiffness_2 - Stiffness_1}{|Stiffnes_1|} \times 100 = \frac{3{,}453 - 3{,}228}{|3{,}228|} \times 100 = 7\% \tag{21}$$

Top of stroke:

$$Stiffness_2 = \frac{F}{\Delta x} = \frac{325}{7.589e^{-2}} = 4{,}283\,\frac{N}{mm} \tag{22}$$

$$\%\ increase_{1-2} = \frac{Stiffness_2 - Stiffness_1}{|Stiffnes_1|} \times 100 = \frac{4{,}283 - 3{,}392}{|3{,}392|} \times 100 = 26\% \tag{23}$$

End of stroke:

$$Stiffness_2 = \frac{F}{\Delta x} = \frac{150}{3.318e^{-2}} = 4{,}521\,\frac{N}{mm} \tag{24}$$

$$\%\ increase_{1-2} = \frac{Stiffness_2 - Stiffness_1}{|Stiffness_1|} \times 100 = \frac{4{,}521 - 3{,}277}{|3{,}277|} \times 100 = 38\% \tag{25}$$

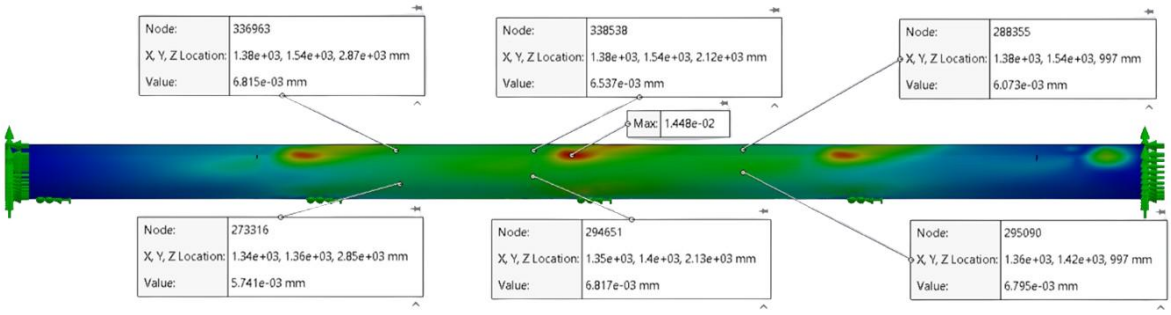

Figure 46. Proposed design: Start of stroke.

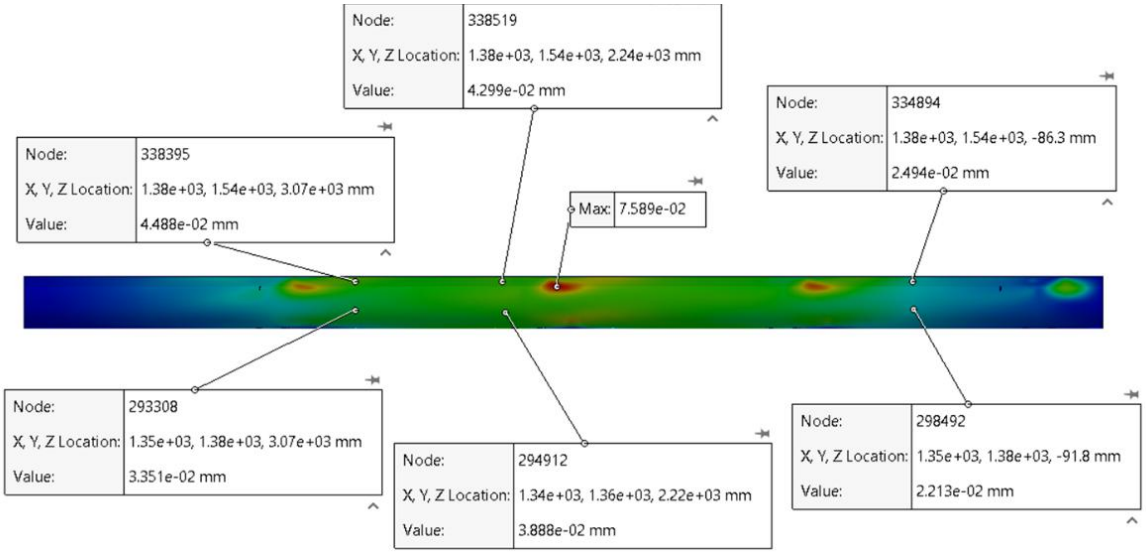

Figure 47. Proposed design: Top of stroke.

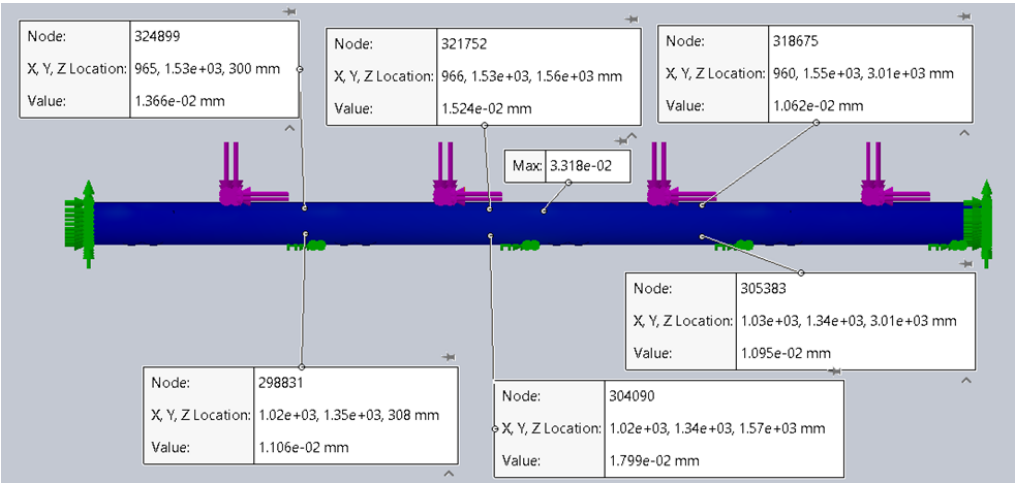

Figure 48. Proposed design: End of stroke.

1.8.5 Simulation 5: Frequency Simulation

1.8.5.1 Frequency Setup

The frequency simulation involves two immovable fixtures on either end of the hull and on the riggers to allow for support while the frequency simulation is run. The supports on the riggers avoid from them being having the highest frequencies, keeping the study focus on the hull. The simulation will replicate the effects of a dynamic environment, replicating the displacement that may take place due to vibration in the shell, showing the areas of weakness of the hull. In this configuration, the resultant frequency study is run at 0.45 Hz which is the natural frequency of the model measured in *Section 1.7.5*. The weaker areas will have higher resonance at this frequency.

1.8.5.2 Frequency Results

The frequency study was only run on the original model to validate the vibration testing completed. The magnitudes in Amps were neglected as the simulation models to not account for the stiffness added by the resin to the boat. This means the magnitudes will differ, however, the trends will remain the same. The heat map and trends were used for validation, and both weak areas were identified in the same area as shown in Figure 49 and Figure 50.

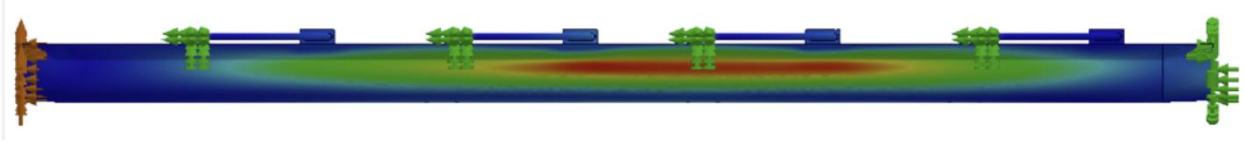

Figure 49. Frequency on model 1.

Figure 50. Heat map from physical vibration test.

1.8.6 Simulation Results

The simulations give stiffness increases across all four simulations. The lowest increase in stiffness is at the point of maximum deflection in the *Start of stroke* simulation. This value gives an increase of only seven percent. While this is below the design target, the model remains stiffer. There are only two more measurement locations – in the same *Start of stroke* study – which give values below the target stiffness. The average stiffness increases for the three rowing simulations are 47%, 51%, and 59%. These values are all much higher than the design targets proving the success of the combined material and dimensional changes. All stiffnesses found in Table 13. Stiffness increases across four simulations. were found using the same calculations from Equations (20) and (21).

The torsional study has one area with a stiffness decrease of 6%, likely due to a difference in the probe placement. This data point is most likely an outlier and is considered as such for this project. All other stiffnesses have very large stiffness increases, the average between all points – including the outlier – being 332%. The values of the torsion in the model are so small that the differences in the models are over-inflating the results. Nevertheless, the new model is shown to have an increase in torsional stiffness over the original design.

These FEA models do not consider the added stiffness the epoxy resin introduces to the model. The increase in stiffness from the resin will be approximately linear for both models. The magnitudes will change but the trends will remain the same. These FEA results show promising improvements to the hull boat. The next steps are to validate the FEA material changes for Fluidesign to implement the design.

Table 13. Stiffness increases across four simulations.

Location	Start of Stroke					Peak of Stroke				
	Original		New		% Increase	Original		New		% Increase
	Disp. (mm)	Stiffness (N/mm)	Disp. (mm)	Stiffness (N/mm)		Disp. (mm)	Stiffness (N/mm)	Disp. (mm)	Stiffness (N/mm)	
1	7.95E-03	6.29E+03	6.82E-03	7.34E+03	**17%**	6.30E-02	5.16E+03	4.49E-02	7.24E+03	**40%**
2	1.34E-02	3.73E+03	6.54E-03	7.65E+03	**105%**	6.47E-02	5.02E+03	4.30E-02	7.56E+03	**51%**
3	1.06E-02	4.72E+03	6.07E-03	8.23E+03	**75%**	3.57E-02	9.11E+03	2.49E-02	1.30E+04	**43%**
4	8.68E-03	5.76E+03	5.74E-03	8.71E+03	**51%**	5.32E-02	6.11E+03	3.35E-02	9.70E+03	**59%**
5	1.09E-02	4.61E+03	6.82E-03	7.33E+03	**59%**	6.42E-02	5.06E+03	3.89E-02	8.36E+03	**65%**
6	7.74E-03	6.46E+03	6.80E-03	7.36E+03	**14%**	3.77E-02	8.63E+03	2.21E-02	1.47E+04	**70%**
Max	1.55E-02	3.23E+03	1.45E-02	3.45E+03	**7%**	9.96E-02	3.26E+03	7.59E-02	4.28E+03	**31%**
Avg.	1.07E-02	4.97E+03	7.61E-03	7.15E+03	**47%**	5.97E-02	6.05E+03	4.05E-02	9.27E+03	**51%**
Location	End of Stroke					Torsion Study				
	Original		New		% Increase	Original		New		% Increase
	Disp. (mm)	Stiffness (N/mm)	Disp. (mm)	Stiffness (N/mm)		Disp. (rad)	Stiffness (Nm/rad)	Disp. (rad)	Stiffness (Nm/rad)	
1	1.96E-02	7.65E+03	1.37E-02	1.10E+04	**44%**	1.35E-02	7.52E+03	3.19E-03	3.18E+04	**323%**
2	3.55E-02	4.23E+03	1.52E-02	9.84E+03	**133%**	1.51E-02	6.74E+03	2.48E-03	4.10E+04	**508%**
3	1.30E-02	1.16E+04	1.06E-02	1.41E+04	**22%**	1.26E-02	8.08E+03	3.23E-03	3.14E+04	**289%**
4	1.90E-02	7.92E+03	1.11E-02	1.36E+04	**71%**	2.04E-04	4.99E+05	2.16E-04	4.71E+05	**-6%**
5	3.14E-02	4.78E+03	1.80E-02	8.34E+03	**74%**	6.41E-04	1.58E+05	7.41E-05	1.37E+06	**766%**
6	1.41E-02	1.07E+04	1.10E-02	1.37E+04	**29%**	8.16E-04	1.24E+05	5.18E-04	1.96E+05	**58%**
Max	4.58E-02	3.28E+03	3.32E-02	4.52E+03	**38%**	1.64E-02	6.21E+03	3.35E-03	3.03E+04	**388%**
Avg.	2.55E-02	7.15E+03	1.61E-02	1.07E+04	**59%**	8.46E-03	1.16E+05	1.87E-03	3.10E+05	**332%**

1.8.7 Validation

Finite Element Analysis (FEA) was used to evaluate the deflection and stiffness of the boat under various loading conditions, helping to identify areas of weakness. However, FEA models are limited by their inability to fully replicate real-world physics, such as the dynamic interaction between the rower and the boat, as well as the hydrostatic forces on the boat. These simplifications can result in discrepancies, particularly in accurately simulating material behaviors and complex loading scenarios. To address this, vibration tests have been conducted. This allows the comparison of the predicted deflection pattern from the simulation with those observed in physical tests. While the magnitude of deflections may differ, ensuring that the deflection patterns align between the FEA model and the physical tests will confirm accuracy of the simulation. From the results, the testing and simulation patterns do align, confirming the accuracy of the FEA patterns.

Further validation will occur in the material testing phase by Fluidesign. Small hull sections—one with the proposed new material and the other with the current material—will be fabricated to directly compare their torsional stiffnesses under controlled vibration and deflection tests. These tests will assess both vibration response and deflection resistance, to confirm the FEA of the material change. This comparison, outlined in *Section 1.10* will validate stiffness improvements due to material choice and validate the accuracy of the FEA model in predicting the real-world performance of the modified hull.

1.9 Project Timing and Delays

Throughout the duration of the capstone project, several unforeseen challenges impacted the original project timeline. The team aimed to complete the FEA of the rowing shell by October 18, 2024, while this deadline was technically met, the process was significantly delayed due to unexpected complications with SolidWorks. Simulating and analyzing the complex geometry of a competition-grade rowing shell proved more intricate than initially anticipated. These issues were resolved through extensive independent research and direct consultation with academic experts and professors experienced in SolidWorks simulation. Simultaneously, initial efforts to conduct strength testing were delayed. The original approach involved constructing a custom accelerometer using piezoelectric sensors and an Arduino. However, difficulties with sensor sensitivity, inconsistent signal readings, and the complexity of integrating the hardware and software rendered this approach unfeasible. As a solution, the team opted to purchase a commercially available Bluetooth tri-axial accelerometer, which streamlined the data collection process significantly.

Additionally, the development of preliminary CAD models, although submitted on time, did not meet the team's quality expectations due to the intricate geometry and lack of prior experience with similar structures. These challenges paralleled those encountered during the FEA process, and were resolved through the same methods of rigorous research and expert consultation. By the time of design review on October 18, 2024, the team had not yet begun material testing. This decision was made intentionally to prioritize finalizing CAD models, improving simulations, and completing the Arduino-accelerometer testing rig. In hindsight, this shift in priority contributed to further timeline setbacks. By the time of the concept design presentation on January 17, 2025, the simulation data had reached the desired state of completeness. However, due to delays in testing setup and material procurement, the team was unable to perform a planned first round of material testing on carbon samples. As a result, this limited the depth of the design analysis available to the judges on that day.

As a cumulative result of the various unforeseen setbacks encountered throughout the project, ranging from technical challenges in simulation and CAD modeling to delays in sensor development and material acquisition, the team was ultimately unable to complete a second round of material testing combined with a third round of vibration testing on a partial section of a hull built from the recommended layup by April 4, 2025. These additional tests were intended to validate simulation results, assess the structural integrity of the design under more realistic conditions, and refine the vibration profile of the boat. However, limitations in both time and available resources prevented their execution. Despite these shortcomings, the team prioritized providing the client with detailed experimental procedures and test protocols to facilitate independent post-project testing, ensuring continuity and usability of the project outcomes beyond the formal completion date. Ultimately, the project still delivered robust insights into performance improvements that Fluidesign could pursue in future iterations of their rowing shells.

Refer to Appendix V for the full MS Project Timeline.

1.10 Future Actions

To extend this stiffness analysis into real-world performance conditions, the next logical step is to test the rowing boat while it is in active use on the water. This will allow the engineering team to observe how the hull dynamically responds to real-time loading conditions such as stroke force, crew weight

distribution, hydrodynamic drag, and wave-impact, factors that static testing cannot fully capture. The core analysis methodology remains the same, but the data gathered during on-water trials provides an added layer of operational relevance that enhances structural insight.

For optimal data collection, tri-axial accelerometers should be mounted at key structural and dynamic locations on the hull. These include the bow near the riggers to capture leading-edge flexure, the stern to monitor tail-end resonance, the midsection (especially under seat 2 or 3) where bending moments are highest due to rower input, and the keel to detect vertical flexure from water impact. Additional sensors under each seat deck beam can help correlate rower mass and footplate pressure with structural response. Ideally, a configuration of 4 to 12 sensors spaced evenly along the target location should be used, and the data should be synchronized to maintain temporal and phase alignment across all points.

During on-water trials, data should be captured during steady-state rowing, high-intensity intervals, sprint starts, and recovery strokes to obtain a broad dynamic range. The use of GPS and stroke rate sensors is also recommended to correlate vibrational data with boat velocity and cadence. Once collected, the data can be processed using the existing Python program with minimal changes. The FFT analysis, stiffness scoring, and spectrogram generation will reveal how the structure behaves under load, highlighting soft zones where vibrational amplitudes are high and stiffness is low. Comparing in-water results to baseline dry-land measurements can help engineers identify load-sensitive compliance, fatigue-prone regions, and shifts in resonance that may indicate material degradation or bonding failure.

Insights drawn from this analysis can inform targeted design improvements. Engineers can modify fiber layup patterns, adjust rib placement, and optimize composite core thickness to mitigate dynamic deflection and enhance energy transfer efficiency. The goal is to shift natural frequencies (currently 0.45 Hz) away from the range of rowing cadence (~0.5-2 Hz) to prevent unwanted resonance. Future enhancements to the system could include the integration of strain gauges or fiber Bragg grating (FBG) sensors for direct deformation measurements, 6-degree-of-freedom IMUs for holistic motion tracking, and wavelet-based signal processing for higher-resolution time-frequency analysis.

Ultimately, in-water stiffness testing transforms raw accelerometer data into actionable engineering decisions, enabling Fluidesign to fine-tune hull performance for speed, durability, and energy efficiency. This iterative, data-driven approach supports elite-level race preparation and ensures that structural optimization aligns directly with the demands of competitive rowing.

1.11 Conclusion

Based on the results from the physical vibration testing, the SolidWorks simulations, and material analysis, the final design of the new quad hull has been successfully completed. The updated design achieves significant improvements in both lateral and torsional stiffness while maintaining weight requirements and accommodating the required dimensional changes. The design requirements have been met, where the width of the gunnel has been reduced to fit the sweep and scull riggers from the double boats. The addition of a new material layup has provided a torsional stiffness increase of approximately 50% and a lateral stiffness improvement of approximately 300%.

During the course of this project, the combination of knowledge from different mechanical courses were combined together and applied to help set up the plan for testing and deriving the final hull design. Teamwork was essential for the productivity of the time spent together, and with the support from

professors and each other the timeline was well planned out and the results for the final design were completed on time. With the final design meeting, all desired expectations and successfully addressing Fluidesign's needs, the next steps allow for Fluidesign to use the final design, with the provided SolidWorks assemblies and drawings, to revise and draw conclusions for the next steps forward. The test plans will also be provided for Fluidesign to take future testing steps for vibration analysis and material tests.

2.0 References

[1] Jones, A. L., et al. "Advancements in Composite Materials for High-Performance Rowing Boats." *Materials Science in Sports Equipment*, vol. 15, no. 2, 2023, pp. 89-101. This article covers carbon fiber-epoxy layering, vacuum bagging, and heat curing processes in racing row boats. www.materialsciencesportseq.com.

[2] Tan, I. "Structural Applications of Honeycomb Core Sandwich Panels in Boat Design." *Journal of Marine Engineering*, vol. 68, no. 4, 2023, pp. 212-227. Details honeycomb core sandwich structures, emphasizing their lightweight and rigid properties for competitive boat designs. www.journalmarinengineering.org.

[3] "Innovations in Rowing Boat Design." *Marine Composites Review*, no. 32, 2022, pp. 35-44. Highlights the use of multiple carbon fiber layers to enhance stiffness, aligned in specific orientations to counteract flexing during heavy rowing loads. www.marinecompositesreview.com.

[4] Richards, M. "Traditional and Modern Stiffening Techniques in Boat Manufacturing." *Rowing Technology Quarterly*, vol. 5, no. 3, 2021, pp. 70-80. Access at www.rowtechquarterly.com.

[5] Delex Change. "Understanding Spars in Aircraft." *Delex Change*, 2024, delexchange.org. Accessed 25 Oct. 2024. Available at www.delexchange.org.

[6] "Commercial Grade Carbon Fiber Fabric 2×2 Twill 3K 6OZ/203GSM - Composite Envisions." *Composite Envisions - Providing The Largest Selection of Composite Fabrics & Materials*, 23 Oct. 2024, compositeenvisions.com/product/commercial-grade-carbon-fiber-fabric-2x2-twill-3k-6oz-203gsm/?srsltid=AfmBOoqdTYHcWdPDlb3hgpqf764zihjNmOoSNFetVymANX36tR9CoFyN.

[7] "West 105B Resin .98 Gallon." *Buy West 105B Resin 0.98 Gallon in Canada Binnacle.Com*, ca.binnacle.com/Maintenance-West-System-Epoxy/c50_306/p3581/West-105B-Resin-.98-Gallon/product_info.html. Accessed 25 Oct. 2024.

[8] "Fainwan 5pcs Piezoelectric Sensor Analog Ceramic Vibration Sensor Module Piezoelectricity Compatible with ARD-Uino DIY Kit." *Amazon.ca: Industrial & Scientific*, www.amazon.ca/gp/product/B09V3C5TXZ/ref=ewc_pr_img_1?smid=A3V3IUEMLKZA8F&psc=1. Accessed 25 Oct. 2024.

[9] "Murrays 100% Pure Australian Beeswax 4 Oz. by Murray's." *Amazon.ca: Home*, www.amazon.ca/gp/product/B00LLJ6Z58/ref=ewc_pr_img_2?smid=AVIMXNFSBIDXU&psc=1. Accessed 25 Oct. 2024.

[10] "Elegoo Upgraded Electronics Fun Kit w/Power Supply Module, Jumper Wire, Precision Potentiometer, 830 Tie-Points Breadboard for Arduino, Raspberry Pi, STM32." *Amazon.ca: Electronics*, www.amazon.ca/gp/product/B01ERPEMAC/ref=ewc_pr_img_1?smid=A2WWHQ25ENKVJ1&psc=1. Accessed 25 Oct. 2024.

[11] "20 Gauge Wire 2 Conductor Electrical Wire, 20 AWG Wire Stranded PVC Cord, 12V Low Voltage/Tinned Copper/Flexible/20/2 Wire for Automotive Wire Led Strips Lamp Lighting Marine

(30ft-9.1m).” Accessed 25 Oct. 2024. *Amazon.ca: Tools & Home Improvement*, 20 Gauge Wire 2 Conductor Electrical Wire, 20 AWG Wire Stranded PVC Cord, 12V Low Voltage/Tinned Copper/Flexible/20/2 Wire for Automotive Wire LED Strips Lamp Lighting Marine (30FT-9.1M) : Amazon.ca: Tools & Home Improvement

[12] “Diagram Defining Horizontal Angular Displacement of the Oar, Where F Is...” *Download Scientific Diagram*, www.researchgate.net/figure/Diagram-defining-horizontal-angular-displacement-of-the-oar-where-F-is-the-boat-The_fig1_328148929. Accessed 10 Jan. 2025.

[13] “Physics of Rowing Oars” *New Journal of Physics*, https://iopscience.iop.org/article/10.1088/1367-2630/ab4226/pdf. Accessed 10 Jan. 2025.

Appendix I: Vibration Testing Manual

This manual details how to set up and execute vibration testing for a static test in which the boat to be tested is set up on a stationary stand and a dynamic test to measure the vibration in water.

The testing equipment used for this test is a WitMotion WT9011DCL sensor, the WitMotion App, and beeswax for temporary attachment of the sensor to the boat hull.

1. Sensor Setup and Use (see WitMotion setup manual for further instruction)

   (a) Push the button on the sensor to turn on ensuring the green light begins flashing. If no light appears, the sensor may be dead and requires charging.

   (b) In the WitMotion app, connect the sensor using instructions in Figure 51.

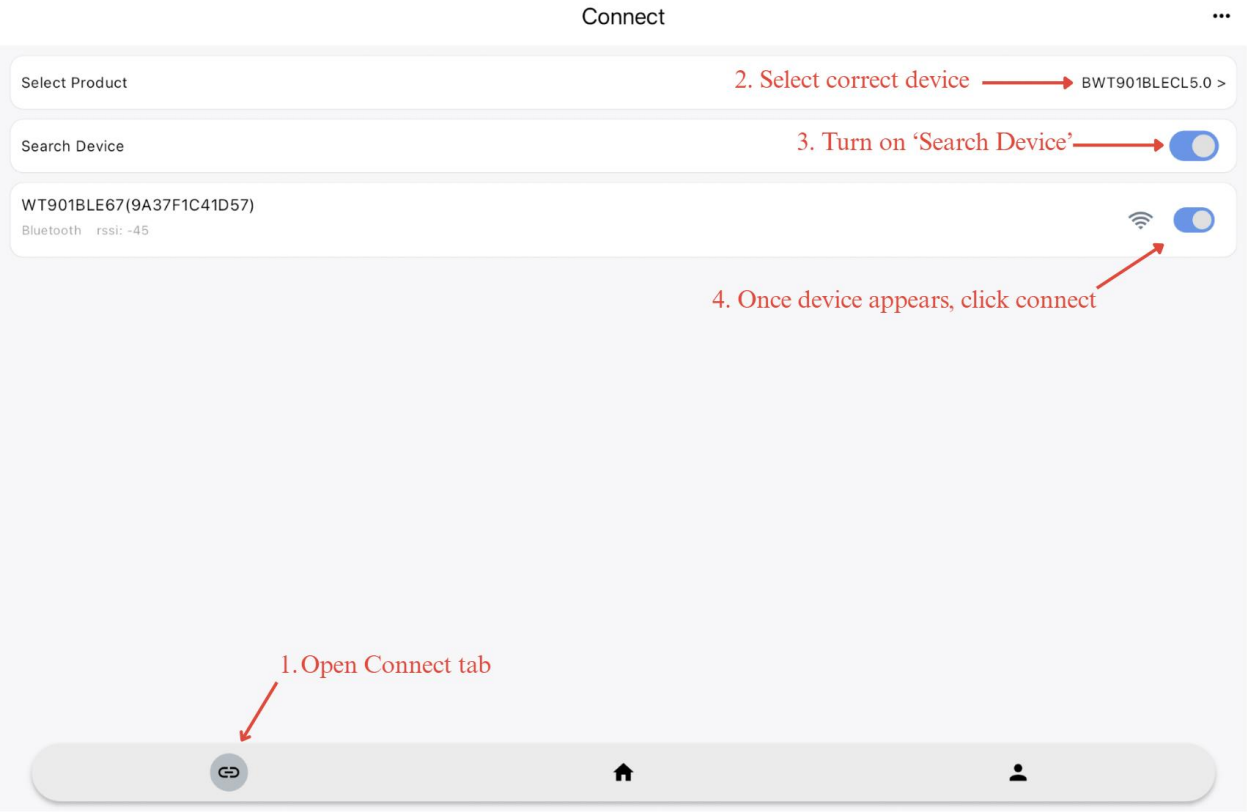

Figure 51. Connecting sensor to device.

   (c) You are now ready to begin recording data. In the home tab, select the acceleration tab at the top of the screen (see Figure 52). There are 5 measurements this sensor can read, but for this test, only acceleration will be measured.

   (d) To start recording data, hit the play button to the right of the screen seen in Figure 52. This is the same button to press to end the recording.

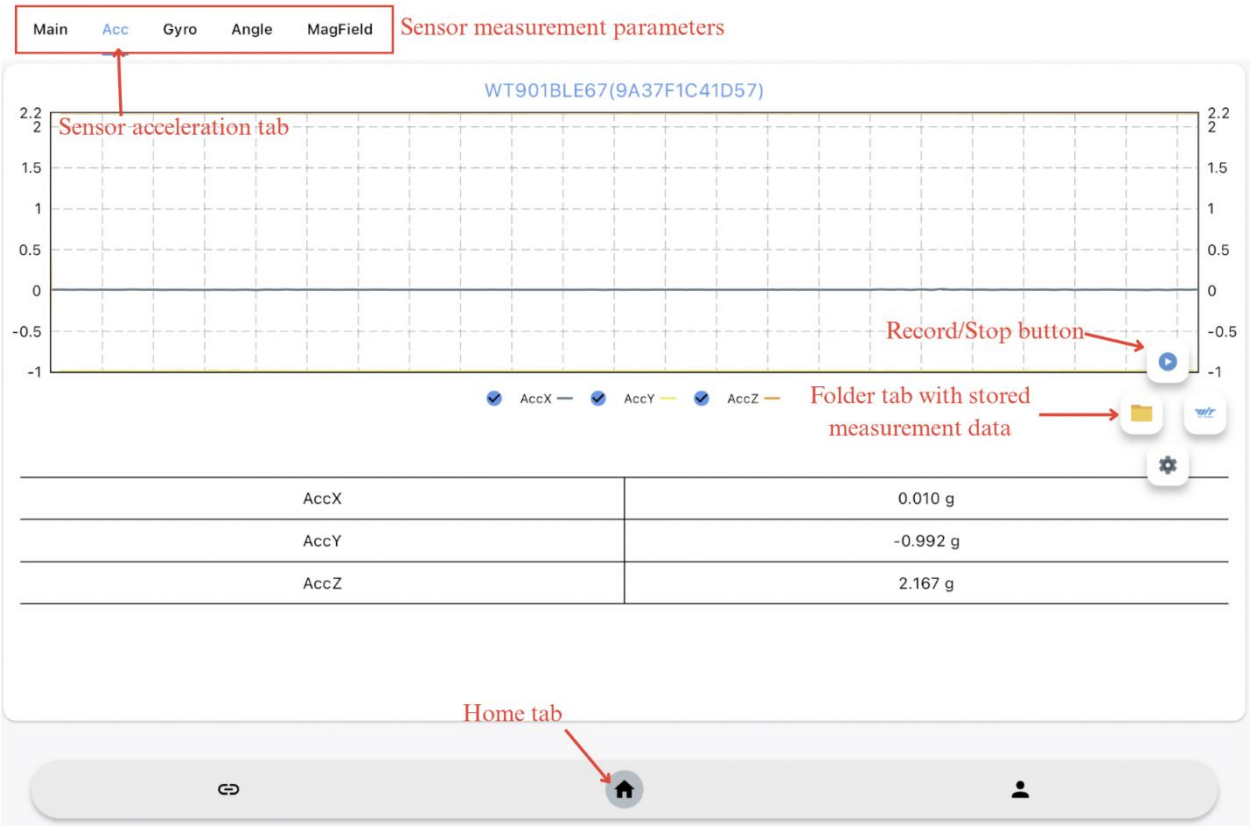

Figure 52. Recording vibration data.

2. Test Setup: Stationary Boat Test

a) For this test, the boat is ideally suspended by the ends to reduce damping from boat stands but stands can also be used.

b) Map test locations either evenly spaced across the boat or concentrated around areas of concern. Figure 53 shows locations used for previous vibration testing.

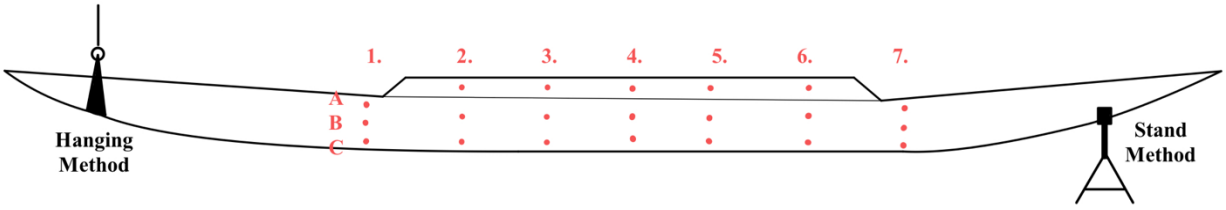

Figure 53. Test location mapping.

c) Apply a small amount of beeswax to each test location to stick the sensor to the hull.

d) Attach sensor to first data point and hit record on WitMotion app. Instructions for this in '1. Sensor Setup and Use'.

e) Impact the boat in one location, keeping the force the same, an example of impact setup below in **Error! Reference source not found.**4.

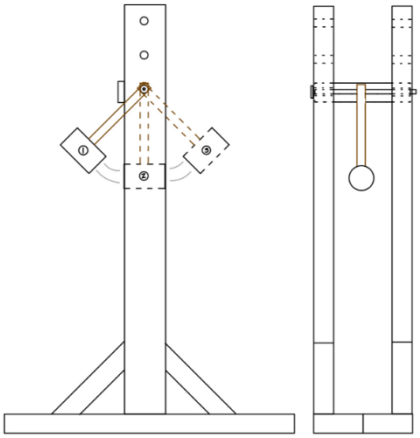

Figure 54. Impact setup.

f) Record the data for roughly ten seconds after impact. Stop recording.

g) Repeat steps ‘e’ and ‘f’ two more times in the same location before moving the sensor to the next location.

h) Measure three impacts per location, measuring all twenty-one locations.

i) Go to section 4 for data exporting and converting.

3. Dynamic Rowing Testing

a) This is a dynamic test to be performed in water with four rowers in the boat.

b) The sensor should always be placed inside the boat as the beeswax may not be strong enough to keep the sensor attached to the boat underwater.

c) Map test locations around the boat where available for placement (between seats, under riggers, an example shown in Figure 55).

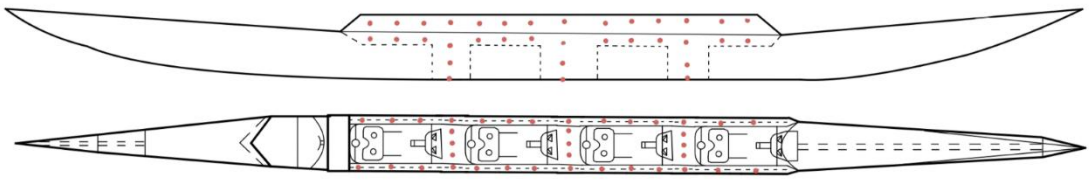

Figure 55. Dynamic test locations.

d) Apply a small amount of beeswax to each location to attach the sensor. Attach the sensor to the first test location.

e) With the sensor turned on and connected and outlined in section 1, hit record.

f) Have the rowers complete three row strokes per reading, rowing in a straight line to reduce errors, then stop the reading.

g) Complete three readings per location, repeating steps ‘e’ and ‘f’. Take readings for every location mapped out.

h) Follow to section 4 for data exporting and converting.

4. Data Exporting and Conversion

a) To export data, each reading needs to be sent from the WitMotion app. To do this, open the files folder in the app, select the folder with the date of the measurements, open each .txt file (one per reading), and export them to a computer via email (see Figure 51 and Figure 56).

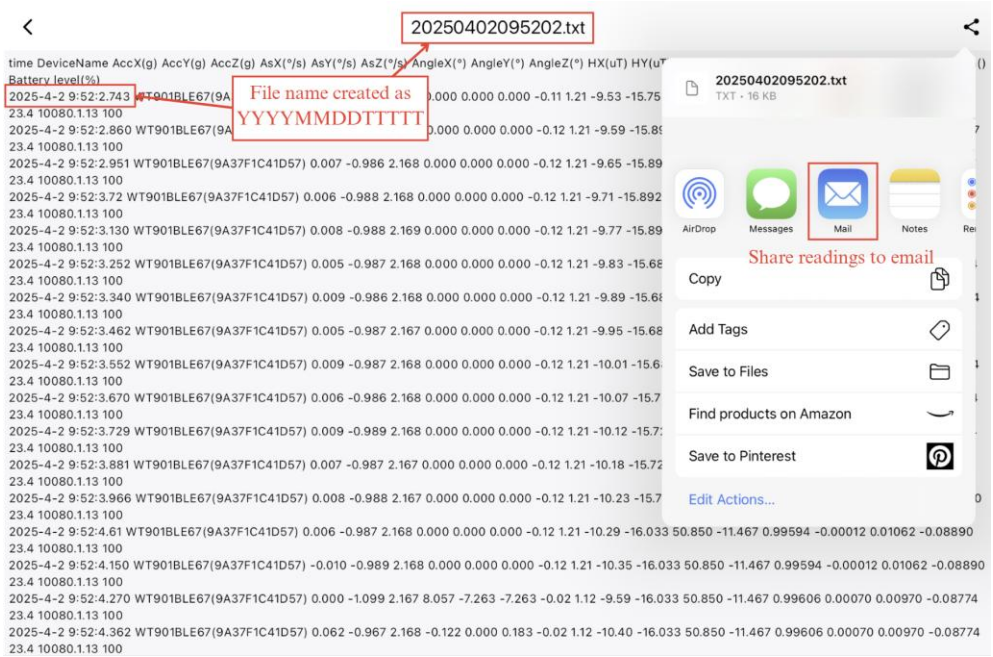

Figure 56. Exporting data from the WitMotion app.

b) Send all recorded files to email. Create an email folder for email files to go into.

c) Run the following codes in order, provided in Appendix II, changing folder names where applicable.

i. Email2File.m – Convert all emailed files to a folder.

d) Rename the folder containing the raw data files to “Raw_Readings”

5. Data Analysis

a) Create a Python script using the code “Stiffness_Analysis.py” in Appendix III using any IDE of your choice.

b) Ensure the Python file is named “Stiffness_Analysis.py” and place it in the same folder containing the raw data

i) Ensure that the ONLY .txt files in this folder are the raw data outputs from MATLAB

c) Run the code

d) A file titled “Analysis” will appear in this folder. Format shown in Figure 57

i) Within the “Analysis” folder should be the files shown in Figure 58.

e) Refer to *Section 1.7.4* for analysis of plots.

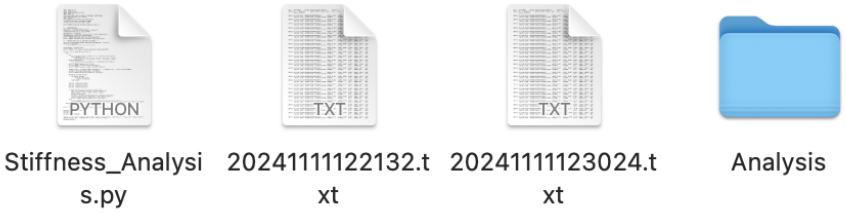

Figure 57. Analysis output files.

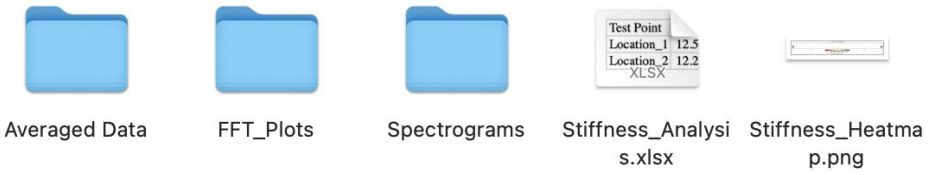

Figure 58. Analysis files.

Appendix II : Matlab Codes

Email2File.m

```
% Create an Outlook application object
outlook = actxserver('Outlook.Application');
mapiNamespace = outlook.GetNamespace('MAPI');

% Access the "BoatFiles" folder within the default mailbox
folders = mapiNamespace.Folders.Item(1).Folders; % Access main account folders
boatFilesFolder = folders.Item('FILENAME'); % Replace "FILENAME" with the exact name of
% your folder

% Define the folder where attachments will be saved
saveFolder = 'OUTPUT FOLDER PATH'; % Replace with output folder name
if ~exist(saveFolder, 'dir')
   mkdir(saveFolder);
end
% Loop through each mail item in the "BoatFiles" folder
numMessages = boatFilesFolder.Items.Count;
for i = 1:numMessages
   mailItem = boatFilesFolder.Items.Item(i);

   % Check if the mail has attachments
   if mailItem.Attachments.Count > 0
      % Loop through each attachment in the email
      for j = 1:mailItem.Attachments.Count
         attachment = mailItem.Attachments.Item(j)
         % Get the original filename and append the order number
         [~, name, ext] = fileparts(attachment.FileName);
         newFileName = sprintf('%s_%d%s', name, i, ext);
         % Save the attachment with the new filename
         attachment.SaveAsFile(fullfile(saveFolder, newFileName));
      end
   end
end
disp('Attachments saved successfully.');
```

Appendix III : Python Code

Stiffness_Analysis.py

```
import numpy as np

import pandas as pd

import matplotlib.pyplot as plt

import glob, os

from scipy.signal import windows, find_peaks, spectrogram

from scipy.fft import fft, fftfreq

import openpyxl

from openpyxl.utils import get_column_letter

from matplotlib import colormaps as cmaps

from mpl_toolkits.mplot3d import Axes3D

print("[DEBUG] Starting stiffness analysis script...")

# --- CONFIGURATION ---

script_dir = os.path.dirname(__file__)

analysis_dir = os.path.join(script_dir, 'Analysis')

os.makedirs(analysis_dir, exist_ok=True)

raw_input_dir = script_dir

avg_output_dir = os.path.join(analysis_dir, 'Averaged Data')

os.makedirs(avg_output_dir, exist_ok=True)


print(f"[DEBUG] Raw input directory: {raw_input_dir}")

print(f"[DEBUG] Averaged output directory: {avg_output_dir}")


# --- COMBINE RAW FILES AS INDIVIDUAL LOCATIONS ---

raw_files = sorted(glob.glob(os.path.join(raw_input_dir, '*.txt')))

for file in raw_files:
```

```
    print(f"[DEBUG] Accepted raw file: {file}")

num_locations = len(raw_files)
print(f"[DEBUG] Total sensor locations detected: {num_locations}")

for loc, file in enumerate(raw_files, 1):
    try:
        try:
            df = pd.read_csv(file, delimiter='\t', encoding_errors='ignore')
            if df.shape[1] <= 1:
                raise ValueError("Tab delimiter failed — switching to comma")
        except Exception as _:
            df = pd.read_csv(file, delimiter=',', encoding_errors='ignore')

        print(f"[DEBUG] Reading file: {file}")
        print(f"[DEBUG] First few rows:\n{df.head()}")
        print(f"[DEBUG] Original columns: {list(df.columns)}")

        columns_clean = [c.strip().lower().replace('\r', '').replace('\n', '') for c in df.columns]
        col_map = dict(zip(columns_clean, df.columns))
        print(f"[DEBUG] Normalized column map: {col_map}")

        def match_col(search_term):
            for key in col_map:
                if search_term in key:
                    return col_map[key]
            return None
```

```
        time_col = match_col('time')
        accx_col = match_col('accx')
        accy_col = match_col('accy')
        accz_col = match_col('accz')

        if all([time_col, accx_col, accy_col, accz_col]):
            data = df[[time_col, accx_col, accy_col, accz_col]]
            data.columns = ['Time', 'AccX', 'AccY', 'AccZ']
            avg_df = data.copy()
            out_path = os.path.join(avg_output_dir, f'Location_{loc}.txt')
            avg_df.to_csv(out_path, index=False, header=False, sep='\t')
            print(f"[DEBUG] Saved averaged data to {out_path}")
        else:
            print(f"[DEBUG] File {file} missing required acceleration/time columns")
            print(f"[DEBUG] Matched columns — Time: {time_col}, AccX: {accx_col}, AccY: {accy_col}, AccZ: {accz_col}")
    except Exception as e:
        print(f"[DEBUG] Failed to read/process {file}: {e}")

print("[DEBUG] Preprocessing complete. Beginning FFT and visualization...")

from openpyxl import Workbook
wb = Workbook()
ws = wb.active
ws.title = "FFT Summary"

headers = ["Test Point", "Freq_X (Hz)", "Amp_X (m/s²)", "Freq_Y (Hz)", "Amp_Y (m/s²)", "Freq_Z (Hz)", "Amp_Z (m/s²)", "Freq_Resultant (Hz)", "Amp_Resultant (m/s²)", "Stiffness Score"]
ws.append(headers)
```

```
output_excel = os.path.join(analysis_dir, "Stiffness_Analysis.xlsx")
output_fft = os.path.join(analysis_dir, "FFT_Plots")
output_spec = os.path.join(analysis_dir, "Spectrograms")
os.makedirs(output_fft, exist_ok=True)
os.makedirs(output_spec, exist_ok=True)

location_files = sorted(glob.glob(os.path.join(avg_output_dir, 'Location_*.txt')))

stiffness_scores = []
positions = np.linspace(0, 1, len(location_files))

for file in location_files:
    name = os.path.basename(file).replace('.txt', '')
    print(f"[DEBUG] Processing {name}...")
    try:
        df = pd.read_csv(file, delimiter='\t', header=None)
        df.columns = ['Time', 'AccX', 'AccY', 'AccZ']
        acc = df[['AccX', 'AccY', 'AccZ']].values
        acc = np.nan_to_num(acc)

        if acc.shape[0] < 2:
            print(f"[DEBUG] {name} skipped: not enough data rows.")
            continue

        fs = 50
        N = acc.shape[0]
        freq = fftfreq(N, 1/fs)[:N//2]
```

```
resultant = np.linalg.norm(acc, axis=1)
signals = [acc[:, 0], acc[:, 1], acc[:, 2], resultant]
fft_peaks = []

for sig in signals:
    amp_spec = (2.0 / N) * np.abs(fft(sig)[:N//2])
    amp_spec[:int(2 * N / fs)] = 0  # filter below 2 Hz
    if np.all(amp_spec < 1e-6):
        fft_peaks.append((0, 0))
        continue
    max_idx = np.argmax(amp_spec)
    fft_peaks.append((freq[max_idx], amp_spec[max_idx]))

fx, ax = fft_peaks[0]
fy, ay = fft_peaks[1]
fz, az = fft_peaks[2]
fr, ar = fft_peaks[3]
stiffness = 1 / (ar + 1e-8)
stiffness_scores.append(stiffness)

ws.append([name, fx, ax, fy, ay, fz, az, fr, ar, stiffness])

fig, ax = plt.subplots()
for i, sig in enumerate(signals):
    amp_spec = (2.0 / N) * np.abs(fft(sig)[:N//2])
    amp_spec[:int(2 * N / fs)] = 0
    ax.plot(freq, amp_spec, label=['X', 'Y', 'Z', 'Resultant'][i])
```

```
    ax.set_xlim(2, 25)
    ax.set_title(f"FFT Spectrum - {name}")
    ax.set_xlabel("Frequency (Hz)")
    ax.set_ylabel("Amplitude (m/s²)")
    ax.legend()
    plt.tight_layout()
    plt.savefig(os.path.join(output_fft, f"{name}_FFT.png"))
    plt.close()

    f_spec, t_spec, Sxx = spectrogram(resultant, fs=fs, nperseg=64, noverlap=48, scaling='spectrum')
    T_spec, F_spec = np.meshgrid(t_spec, f_spec)

    print(f"[DEBUG] Spectrogram time range: {t_spec.min():.2f}s to {t_spec.max():.2f}s")
    print(f"[DEBUG] Spectrogram frequency range: {f_spec.min():.2f}Hz to {f_spec.max():.2f}Hz")

    fig_spec = plt.figure(figsize=(10, 6))
    ax_spec = fig_spec.add_subplot(111, projection='3d')
    ax_spec.plot_surface(T_spec, F_spec, np.sqrt(Sxx), cmap='viridis_r', edgecolor='k', linewidth=0.2, antialiased=True)
    ax_spec.set_xlim(0, t_spec.max())
    ax_spec.set_ylim(2, 25)
    ax_spec.set_xlabel('Time [s]')
    ax_spec.set_ylabel('Frequency [Hz]')
    ax_spec.set_zlabel('Amplitude')
    ax_spec.set_title(f"3D Spectrogram - {name}")
    fig_spec.tight_layout()
    plt.savefig(os.path.join(output_spec, f"{name}_Spectrogram.png"))
    plt.close()
```

```
    except Exception as e:
        print(f"[DEBUG] Failed FFT on {name}: {e}")

if stiffness_scores:
    print("[DEBUG] Generating heatmap...")
    normalized = (np.array(stiffness_scores) - min(stiffness_scores)) / (max(stiffness_scores) - min(stiffness_scores) + 1e-8)
    colors = cmaps['RdYlGn'](normalized)

    fig, ax = plt.subplots(figsize=(12, 2))
    for i, pos in enumerate(positions):
        ax.plot([pos], [1], marker='s', markersize=20, color=colors[i], markeredgecolor='k')
        ax.text(pos, 1.05, f"P{i+1}", ha='center', fontsize=8)
    ax.set_xlim(0, 1)
    ax.set_ylim(0.9, 1.2)
    ax.set_yticks([])
    ax.set_title("Stiffness Heatmap")
    ax.set_xlabel("Normalized Boat Length")
    sm = plt.cm.ScalarMappable(cmap=cmaps['RdYlGn'], norm=plt.Normalize(vmin=min(stiffness_scores), vmax=max(stiffness_scores)))
    sm.set_array([])
    cbar = fig.colorbar(sm, ax=ax, orientation='horizontal')
    cbar.set_label('Relative Stiffness Score')
    plt.tight_layout()
    plt.savefig(os.path.join(analysis_dir, "Stiffness_Heatmap.png"))
    plt.close()
    print("[DEBUG] Heatmap saved.")
else:
```

```
    print("[DEBUG] No valid stiffness scores calculated. Skipping heatmap generation.")


wb.save(output_excel)

print(f"[DEBUG] FFT analysis complete. Results saved to: {output_excel}")
```

Appendix IV : Additional Images

time	DeviceName Version()	AccX(g)	AccY(g)	AccZ(g)	AsX(°/s)	AsY(°/s)	AsZ(°/s)	AngleX(°)	AngleY(°)	AngleZ(°)	HX(uT)	HY(uT)	HZ(uT)	Q0()	Q1()	Q2()	Q3()	Temperature(°C) Battery level(%)
2024-11-11 12:21:32.97 10080.1.13	WT901BLE67(BFF45591D575) 100	-0.049	0.988	-0.088	0.000	0.000	0.000	94.97	2.92	-126.39	-1.342	-62.533	8.100	0.28754	0.34778	-0.65002	-0.61133	22.6

Figure 59. Raw data measured by accelerometer.

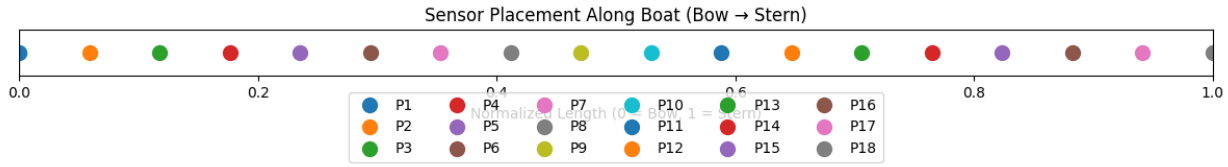

Figure 60. Sensor heat map diagram.

Appendix IV : SolidWorks Material Data

Name	Weave	Thickness (inches)	Weight (oz/yd^2)	Tensile Strength (ksi)		Tensile Modulus (msi)		Brand	Code	Cost ($/yd)
3K Carbon Multifilament Continuous Tow	2 x 2 Twill	0.012	5.7	635		34.9		Fibre Glast	1069	50.95
6K 2x2 Twill Weave Carbon Fiber Fabric	2 x 2 Twill	0.017	10.9	600		35.4		Fibre Glast	1073	69.95
12K 2x2 Twill Weave Carbon Fiber Fabric	2 x 2 Twill	0.03	19.8	655		34.4		Fibre Glast	1072	80.95
3K Plain Weave Carbon Fiber Fabric	Plain	0.012	5.4	635		34.9		Fibre Glast	530	49.95
5HS Weave Carbon Fiber Fabric	5HS	0.024	10.9	700		34.9		Fibre Glast	660	65.95
1K Plain Weave Ultralight Carbon Fiber Fabric	Plain	0.009	3.5	635		34.9		Fibre Glast	2363	184.95
Unidirectional Carbon Fiber	Unidirectional	0.014	9	850	485	41.5	24.5	Fibre Glast	2583	18.95
IM Unidirectional Carbon Fabric	Unidirectional	0.006	4.3	850	485	41.5	24.5	Fibre Glast	2596	18.95
Unidirectional Carbon Fabric (4.0 oz)	Unidirectional	0.006	4	725		34.1		Fibre Glast	2585	8.95
Unidirectional Carbon Fabric (22.3 oz)	Unidirectional	0.03	22.3	725		34.1		Fibre Glast	2595	43.95

Name	Elastic Modulus in X	Elastic Modulus in Y	Elastic Modulus in Z	Poisson's Ratio in XY	Poisson's Ratio in YZ	Poisson's Ratio in XZ	Shear Modulus in XY	Shear Modulus in YZ	Shear Modulus in XZ	Mass Density	Tensile Strength in X	Tensile Strength in Y	Yield Strength
	N/m^2	N/m^2	N/m^2				N/m^2	N/m^2	N/m^2	kg/m^3	N/m^2	N/m^2	N/m^2
3K Carbon Multifilament Continuous Tow	2.41E+11	2.41E+11	8.50E+09	3.00E-01	1.80E-01	1.80E-01	9.20E+10	3.50E+09	3.50E+09	6.34E+02	4.38E+09	4.38E+09	3.06E+09
6K 2x2 Twill Weave Carbon Fiber Fabric	2.44E+11	2.44E+11	8.50E+09	3.00E-01	1.80E-01	1.80E-01	9.20E+10	3.50E+09	3.50E+09	8.56E+02	4.14E+09	4.14E+09	2.90E+09
12K 2x2 Twill Weave Carbon Fiber Fabric	2.37E+11	2.37E+11	8.50E+09	3.00E-01	1.80E-01	1.80E-01	9.20E+10	3.50E+09	3.50E+09	8.81E+02	4.52E+09	4.52E+09	3.16E+09
3K Plain Weave Carbon Fiber Fabric	2.41E+11	2.41E+11	8.50E+09	3.00E-01	1.80E-01	1.80E-01	9.20E+10	3.50E+09	3.50E+09	6.01E+02	4.38E+09	4.38E+09	3.06E+09
5HS Weave Carbon Fiber Fabric	2.41E+11	2.41E+11	8.50E+09	3.00E-01	1.80E-01	1.80E-01	9.20E+10	3.50E+09	3.50E+09	6.06E+02	4.83E+09	4.83E+09	3.38E+09
1K Plain Weave Ultralight Carbon Fiber Fabric	2.41E+11	2.41E+11	8.50E+09	3.00E-01	1.80E-01	1.80E-01	9.20E+10	3.50E+09	3.50E+09	5.19E+02	4.38E+09	4.38E+09	3.06E+09
Unidirectional Carbon Fiber	2.86E+11	1.69E+11	6.50E+09	2.70E-01	1.50E-01	1.50E-01	5.00E+10	2.50E+09	2.50E+09	8.58E+02	5.86E+09	3.34E+09	4.10E+09
IM Unidirectional Carbon Fabric	2.86E+11	1.69E+11	6.50E+09	2.70E-01	1.50E-01	1.50E-01	5.00E+10	2.50E+09	2.50E+09	9.57E+02	5.86E+09	3.34E+09	4.10E+09
Unidirectional Carbon Fabric (4.0 oz)	2.35E+11	1.69E+11	6.50E+09	2.70E-01	1.50E-01	1.50E-01	5.00E+10	2.50E+09	2.50E+09	8.90E+02	5.00E+09	3.34E+09	3.50E+09
Unidirectional Carbon Fabric (22.3 oz)	2.35E+11	1.69E+11	6.50E+09	2.70E-01	1.50E-01	1.50E-01	5.00E+10	2.50E+09	2.50E+09	9.92E+02	5.00E+09	3.34E+09	3.50E+09

Appendix V : Project Timeline

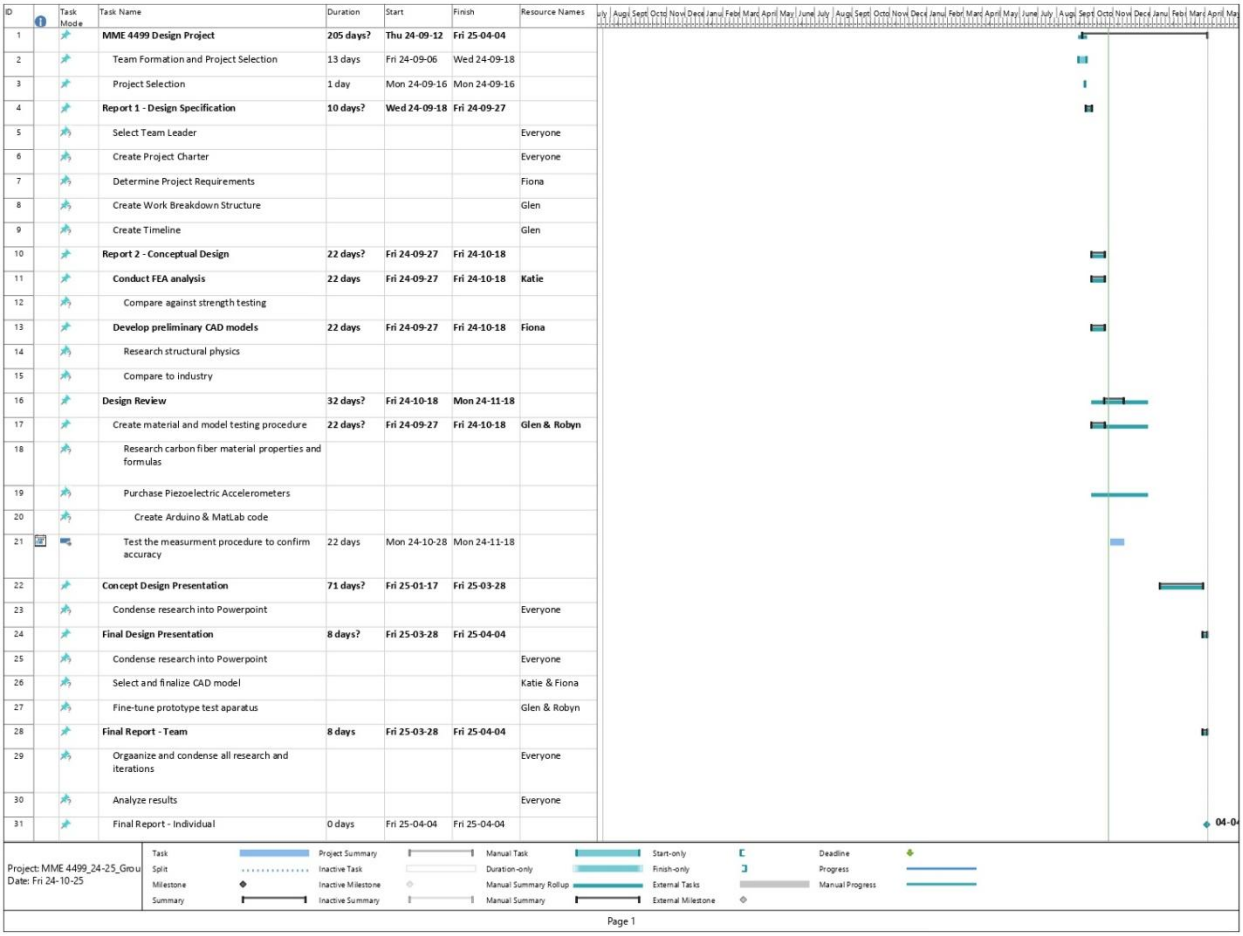

ID	Task Mode	Task Name	Duration	Start	Finish	Resource Names
1		**MME 4499 Design Project**	**205 days?**	**Thu 24-09-12**	**Fri 25-04-04**	
2		Team Formation and Project Selection	13 days	Fri 24-09-06	Wed 24-09-18	
3		Project Selection	1 day	Mon 24-09-16	Mon 24-09-16	
4		**Report 1 - Design Specification**	**10 days?**	**Wed 24-09-18**	**Fri 24-09-27**	
5		Select Team Leader				Everyone
6		Create Project Charter				Everyone
7		Determine Project Requirements				Fiona
8		Create Work Breakdown Structure				Glen
9		Create Timeline				Glen
10		**Report 2 - Conceptual Design**	**22 days?**	**Fri 24-09-27**	**Fri 24-10-18**	
11		**Conduct FEA analysis**	**22 days**	**Fri 24-09-27**	**Fri 24-10-18**	**Katie**
12		Compare against strength testing				
13		**Develop preliminary CAD models**	**22 days**	**Fri 24-09-27**	**Fri 24-10-18**	**Fiona**
14		Research structural physics				
15		Compare to industry				
16		**Design Review**	**32 days?**	**Fri 24-10-18**	**Mon 24-11-18**	
17		Create material and model testing procedure	**22 days?**	**Fri 24-09-27**	**Fri 24-10-18**	**Glen & Robyn**
18		Research carbon fiber material properties and formulas				
19		Purchase Piezoelectric Accelerometers				
20		Create Arduino & MatLab code				
21		Test the measurment procedure to confirm accuracy	22 days	Mon 24-10-28	Mon 24-11-18	
22		**Concept Design Presentation**	**71 days?**	**Fri 25-01-17**	**Fri 25-03-28**	
23		Condense research into Powerpoint				Everyone
24		**Final Design Presentation**	**8 days?**	**Fri 25-03-28**	**Fri 25-04-04**	
25		Condense research into Powerpoint				Everyone
26		Select and finalize CAD model				Katie & Fiona
27		Fine-tune prototype test aparatus				Glen & Robyn
28		**Final Report - Team**	**8 days**	**Fri 25-03-28**	**Fri 25-04-04**	
29		Orgaanize and condense all research and iterations				Everyone
30		Analyze results				Everyone
31		Final Report - Individual	0 days	Fri 25-04-04	Fri 25-04-04	